

re
se
a
r
c
h



NYLE LABORATORIES
TESTING DIVISION, HUNTSVILLE FACILITY

N70-23282

(ACCESSION NUMBER)

(THRU)

45

1

NASA-CR-102.579

(CODE)

02

(NASA CR OR TXR OR AD NUMBER)

(CATEGORY)

FACILITY FORM 408



research

CR-102579

WYLE LABORATORIES - RESEARCH STAFF
REPORT WLR 70-4

SOME APPLICATIONS OF JET NOISE THEORY

By
M.V. Lawson
and
S.P. Pao

Work Performed Under Contract NASS-21060

February 1970



WYLE LABORATORIES
RESEARCH DIVISION, HUNTSVILLE FACILITY

COPY NO. 14

SUMMARY

Results from existing theories for jet noise are critically reviewed for their practical inferences, and they are applied to some practical problems. Shear noise is found to produce half the sound power but double the peak sound pressure of self noise. By means of the Pao-Lawson theory and a set of new aerodynamic data for a low speed jet exhaust flow, the absolute magnitude of self noise source intensity distribution in a jet is calculated. The axial variation of source strength shows almost constant effectiveness (x^0 law) over the initial mixing region with a shallow peak near the end of the potential core. Significant noise radiation occurs down to ten diameters from the exit, with similarity conditions (x^{-7} law) applying only beyond about fifteen diameters. Nearly sixty percent of the noise is found to be radiated from the region of the jet downstream of the potential core. An empirical relation between shear and turbulent intensity suggests that the results are equally applicable to shear and self noise, at least in the initial region. Integration of local source strength over the whole jet gives a theoretical value of the Lighthill parameter for jet noise as 3.3×10^{-5} in comparison with the empirical value of 3×10^{-5} for low speed jets. The spectrum of the overall noise for a low speed jet has also been evaluated. The peak noise is found near a Strouhal number of 0.30. The predicted spectral shape is in close agreement with experiment. The success of the present work demonstrates that the local variations of the gross parameters such as turbulence intensity and scale dominant noise outputs and that detail considerations of wave-number frequency spectra are of secondary importance.

The convection directivity factor, which is independent of the local noise generation mechanism according to Lighthill's formulation, is evaluated for various shear noise and self noise patterns as a function of Mach number. General trends of the U^8 -law in low Mach number range and the U^6 -law for high Mach number range are observed. Abnormalities are found in the transonic range. Application to high speed flows results in prediction of sound power level much larger than values which experimental data would allow. This can be partly explained by aerodynamic source strength arguments, but also results from the neglect of refraction and nonlinear attenuation in the present study. Suggestions are made for aerodynamic and acoustic experiments to further define source mechanisms, so that a theoretically sound prediction method can be specified. A feasible model for the scale ratio in a jet suggests that sound power is proportional to turbulence intensity to the eighth power. This result could be significant in determining the mechanisms underlying jet noise silencing devices.

TABLE OF CONTENTS

	Page
SUMMARY	ii
TABLE OF CONTENTS	iii
LIST OF FIGURES	iv
1.0 INTRODUCTION	1
2.0 INFERENCES FROM THEORY	2
3.0 NOISE SOURCE LOCATION IN A JET EXHAUST	7
4.0 CALCULATION OF THE FREQUENCY SPECTRUM	11
5.0 EXTENSIONS TO THE SUPERSONIC CASE	13
6.0 LIMITATIONS	15
7.0 EXPERIMENTAL RECOMMENDATIONS	17
8.0 EFFECT OF THE SCALE RATIO	20
9.0 CONCLUSIONS	22
REFERENCES	24

LIST OF FIGURES

Figure		Page
1	<p>Spherical Average of the Self Noise Convection Factor,</p> $\frac{1}{4\pi} \int_0^{2\pi} C^{-5} \sin \theta d\theta, \text{ in dB Relative to its Value at Zero Mach}$ <p>Number for each Given Set of Parameters α^2 and ϵ^2 .</p>	26
2	<p>Spherical Average of the Shear Noise Convection and Directivity</p> <p>Factor, $\frac{1}{4\pi} \int_0^{2\pi} C^{-n} \Phi(\theta) \sin \theta d\theta$, in dB Relative to its Value</p> <p>at Zero Mach Number for Each Case of Given n and $\Phi(\theta)$. The Parameters α^2 and ϵ^2 have a Fixed Value of 0.1.</p>	27
3	<p>The Self Noise Convection Directivity Factor at Various Mach Numbers. Sound Pressure Levels are Shown in dB Relative to the Average Sound Pressure Level at Zero Mach Number.</p>	28
4	<p>The Ribner-Pao-Lawson Shear Noise Convection Directivity Factor at Various Mach Numbers. Sound Pressure Levels are Shown in dB Relative to the Average Sound Pressure Level at Zero Mach Number.</p>	29
5	<p>Mean Flow Velocity Profile, Turbulence Intensity Profile, and the Square of their Product at Various Stations along the Axis of a Low Speed Jet Exhaust Flow.</p>	30
6	<p>Contours of Noise Source Intensity in a Low Speed Jet Exhaust Stream. The Intensity Levels are shown in dB Relative to the Maximum Noise Intensity.</p>	31
7	<p>Contours of Local Mean Velocities in a Low Speed Jet Exhaust Stream. The Mean Velocity is Normalized Against the Jet Exhaust Velocity.</p>	32
8	<p>The Integrated Noise Source Strength Per Unit Length Along the Axis of a Low Speed Jet Exhaust Stream.</p>	33
9	<p>Profiles of Maximum Mean Flow Velocity and Maximum Turbulence Intensity in the Axial Direction of the Jet. The Approach to Similarity Assumes Different Patterns for These Profiles.</p>	34

LIST OF FIGURES (Continued)

Figure		Page
10	Subdivision of a Low Speed Jet Exhaust Stream According to the Local Peak Noise Frequency. The Difference Between Peak Frequencies in Consecutive Segments is One-Third Octave.	35
11	The Normalized One-Third Octave Band Spectral Level of the Model "Weighted Gaussian" Frequency Function.	36
12	The Predicted Self Noise, Shear Noise, and Overall Noise Spectra for a Low Speed Jet Based on the Pao-Lowson Theory.	37
13	The Value of $\frac{1}{4\pi} \int_0^{2\pi} \alpha^4 C^{-5} \sin \theta d\theta$, in dB Relative to its Value at Zero Mach Number for Each Given Value of α^2 . The Parameter ϵ^2 has a Fixed Value of 0.1.	38
14	The Two Types of Frequency Spectrum Shows on Normalized Plot.	39
15	Masking and Apparent Reversal of the Curve Non-Associated Doppler Shift Illustrated with Experimentally Derived Data.	40

1.0 INTRODUCTION

The noise from jet and rocket exhausts still represents one of the most significant acoustic sources. It is a major cause of community annoyance, particularly for the projected supersonic transports, and can even cause local structural failure via acoustic fatigue. Furthermore, its characteristics and basic mechanisms are even now not properly understood.

The theory of Lighthill (References 1-4) gave the fundamental description of the noise generation process. Unfortunately utilization of this theory to date has been limited to simple dimensional arguments. Ffowcs-Williams (Reference 5) extended the theory to the supersonic case and recently Pao and Lawson (Reference 6) were able to offer some additional theoretical insight via a spectral approach. However, there has been remarkably little attempt to study the application of the theory to practical conditions. Simple dimensional arguments seem to be the high point of theoretical achievement. Lilley (Reference 7) performed an initial application over ten years ago. The most useful recent work has been that of Ribner, et al., at the Institute for Aerospace Studies, University of Toronto, who have published a series of papers (References 8-12) of increasing practical relevance. Nevertheless, much of the theory remains unapplied.

A second cause of the lack of understanding of jet noise is the lack of systematic and properly analyzed experimental data. Many limited studies have been performed, but most data are unavailable to the typical investigator because of various proprietary restrictions. Lee, et al., report (Reference 13) is perhaps the best one published. But even given the data, very little proper analysis has been performed. Typical data collapses show variations of ± 5 dB so that accurate predictions are not often possible. One reason for this is that virtually all collapses have been empirical. Theory does suggest several methods for data analysis, and it is surprising that such analyses have not been performed. Recently MacGregor and Lush have carried out work along these lines, reported in References 12 and 14, respectively. Their results do show cause for optimism about theoretical approaches to acoustic data analysis.

This report is an attempt to fill in some of the gaps in the practical application of the theoretical results. Section 2.0 discusses basic mechanisms and shows results of some limited parameter studies based on the theory by Pao and Lawson. Section 3.0 combines the Pao-Lawson theory with experimental data to demonstrate the principal noise sources in a jet exhaust and Section 4.0 discusses the noise spectrum predicted on the same basis. Sections 5.0 and 6.0 discuss extensions of the applications to the supersonic case and their limitations. Section 7.0 gives some suggested experiments and data analysis methods which will enable reliable prediction techniques to be developed. Section 8.0 discusses the effects of different assumptions about the scale ratio. Conclusions of this study are summarized in Section 9.0.

2.0 INFERENCES FROM THEORY

The generation of noise by a jet exhaust is basically the result of complex unsteady flow conditions within the jet, which, in a general sense, may be grouped under the description "turbulence". Jet noise theories suggest two primary noise generation processes. The first is referred to as the "self noise" of the jet and the second as the "shear Noise". The "self noise" results from turbulence-turbulence interaction, whereas the shear noise results from the interaction of turbulence with the mean flow of the jet.

There is universal theoretical agreement about the form of the expression for the self noise of the jet. Fao and Lawson (Reference 6) give the following result for the overall noise intensity per unit jet volume resulting from self noise.

$$I(x_0) = \frac{3 \sqrt{2\pi} \rho u_0^4 \alpha^4 M^4}{8 a c r^2 \{(1 - M \cos \theta)^2 + \alpha^2 M^2\}^{5/2}} \quad (1)$$

where

- ρ = atmospheric density
- u_0 = turbulence intensity
- α = dimensionless ratio of space to time scales
- M = convection Mach number
- a = spatial scale
- c = speed of sound
- r = distance from jet
- θ = angle from the jet axis.

Equation (1) was derived on the basis of several assumptions using an isotropic Gaussian form for the wave number and frequency spectra, and making no allowance for the local variation of aerodynamic parameters in the exhaust flow. The numerical constants given depend on these assumptions. But the basic dimensional dependence is identical to that found by Ffowcs-Williams (Reference 5) and Ribner (Reference 8) so that Equation (1) can be used as a basis for discussion of the self noise generation.

Because the self noise is the result of a random assemblage of quadrupoles, it has no preferred direction of radiation. The basic spherical shape is distorted only by the convection factor $C = [(1 - M \cos \theta)^2 + \alpha^2 M^2]^{1/2}$, raised to the -5 power in Equation (1). This convection factor plays a fundamental role in aerodynamic noise theory, and also gives the Doppler frequency shift due to convection, as will be discussed later.

If Equation (1) is integrated over all space, the result is an expression for overall sound power. The only spatial dependence is in the C term and Figure 1 gives the integrated value of this self-noise term over the sphere. In fact, if the real anisotropic nature of turbulence is taken into account, the convection term becomes, as shown by Ffowcs-Williams (Reference 5)

$$C^2 = (1 - M \cos \theta)^2 + \alpha^2 M^2 (\cos^2 \theta + \epsilon^2 \sin^2 \theta) \quad (2)$$

where ϵ is the ratio of the lateral to longitudinal turbulence scales. Figure 1 gives the result of integrating C^{-5} for various values of α^2 and ϵ^2 . The case $\epsilon^2 = 1$ corresponds to an isotropic structure while $\epsilon^2 = 0.1$ is closer to the indicated experimental anisotropy factor. A value of $\alpha^2 = 0.1$ is indicated from subsonic turbulence experiments, and a value of $\alpha^2 = 0.4$ has also been included to indicate the effect of variation of the space to time scales in the turbulence.

Figure 1 shows a M^0 variation at low convection Mach numbers and a M^{-5} variation at high Mach numbers in all cases. This corresponds to the well known U^8 variation at low exhaust speeds and U^3 at high exhaust speeds. The existence of a peak in the overall efficiency near $M_c = 1$ is also a well-known theoretical effect, but this has not been observed in experiment. The apparent non-existence of this peak certainly justifies further study, as will be discussed in more detail later.

Figure 2 shows equivalent results for the shear noise case. Several different results for shear noise directivity exist. Pao and Lawson (Reference 6) give

$$I(x) = \left(\frac{\partial U_1}{\partial x_2} \right)^2 \frac{3 \sqrt{\pi} \rho u_0^2 M^4 \alpha (\cos^4 \theta + \cos^2 \theta)}{16 \pi^2 c r^2 \{ (1 - M \cos \theta)^2 + \alpha^2 M^2 \}^{5/2}} \quad (3)$$

Here $(\partial U_1 / \partial x_2)$ is the mean shear. The basic directionality factor is

$$(\cos^4 \theta + \cos^2 \theta) / 2 C^5 \quad (4)$$

This term agrees with that found by Ribner (Reference 8). Figure 2 shows the result of integrating this term at various Mach numbers. As in the self noise case, Equation (3) was derived from an isotropic model. An anisotropic model would have the C factor given in Equation (2). Figure 2 gives results only for the practical anisotropic case $\alpha^2 = 0.1$, $\epsilon^2 = 0.1$. The effects of change of scale factors α and ϵ would be qualitatively similar to those shown in Figure 1.

A second curve on Figure 2 gives the result for an assumed shear noise dependence

$$\cos^2 \theta / C^3 \quad (5)$$

This differs by a factor of $(1 + \cos^2 \theta)/C^2$ from Equation (4). The basic result of Equation (3) came from assuming a wave number spectrum varying as k at small values of k . This is reasonable for homogeneous turbulence, but for intermittent turbulence a spectrum with constant level at small k could be more appropriate. This would give the result of Equation (5).

The third curve in Figure 2 is for the Lighthill (Reference 2) shear prediction

$$\sin^2 2\theta / C^3 \quad (6)$$

as recently corrected by Jones (Reference 15). The reasons for the differences between Lighthill's directivity and the present have not been fully evaluated, so that the curve is included in Figure 2 for completeness.

Noise from a real jet is a combination of both shear and self noise. Equations (1) and (3) define the sound power dependence as

$$I_{\text{self}} \sim \frac{u_0^4 M^4 \alpha^4}{a} \quad (7)$$

and

$$I_{\text{shear}} \sim \left(\frac{\partial U}{\partial x_2} \right)^2 a u_0^2 M^4 \alpha^4 \quad (8)$$

with the constants and directivity factors omitted from the original equations. Davies, et al. (Reference 16) discovered the following important empirical relation between the turbulence intensity, scale and shear.

$$u_0 = 0.2 a \left(\frac{\partial U}{\partial x_2} \right) \quad (9)$$

This equation was found to hold locally over all the jet except well beyond the core. Equation (9) suggests an interesting conclusion about the shear noise. By virtue of Equation (9), the shear noise dependence becomes

$$I_{\text{shear}} \sim \frac{u_0^4 M^4 \alpha^4}{a}$$

that is, identical with the self noise. Thus, the shear noise and self noise power have exactly the same dependence on local parameters in a jet if the empirical relation of Davies, et al. can be assumed to hold. However, it should be noted that the proportion of the sound power and the directivity patterns of the self and the shear noise remain different.

Dividing Equation (3) by Equation (1) gives the ratio of the shear noise to the self noise

$$\frac{\text{Shear Noise}}{\text{Self Noise}} = \frac{\left(\frac{\partial U}{\partial x_2}\right)^2 \left(\frac{\cos^4 \theta + \cos^2 \theta}{2}\right) a^2}{\sqrt{2} \bar{u}_0^2 x^2} \quad (10)$$

or, on integration to remove the directivity,

$$\frac{\text{Shear Noise Power}}{\text{Self Noise Power}} = \frac{4 a^2}{15 \sqrt{2} x^2 \bar{u}_0^2} \left(\frac{\partial U}{\partial x_2}\right)^2 \quad (11)$$

Values for the aerodynamic parameters are chosen to be characteristic of those of the maximum shear region in a low velocity jet. Taking

$$a = 1.13 L_x = 0.147 x_1 \quad (*)$$

$$\frac{\partial U}{\partial x_2} = \frac{U}{0.16 x_1}$$

$$\bar{u}_0 = 0.16 U$$

gives the characteristic ratio of shear noise power to self noise power as 0.65. The ratio of intensity from Equation (10) is $2.43 \left\{ (\cos^4 \theta + \cos^2 \theta) / 2 \right\}$. Ribner (Reference 9) and Lilley (Reference 7) effectively took the level of self and shear noise to be equal. MacGregor (reported in Reference 12) has found a factor of about 2 in sound pressure level from an empirical data analysis.

(*) The spatial scale a is taken as the spherical average of the longitudinal and lateral scales of an actual turbulence structure. Lawrence (Reference 17) found that the longitudinal scale L_x varies as $L_x = 0.13 x_1$. The lateral scales are about one-third of this value. The spherical average of the spatial scale is therefore $L_{sve} = 0.539 L_x$. The spatial scale a in this report is related to L_{sve} by $a = \sqrt{3} L_{sve}$, due to differences in definition. Hence, the final value for a is $1.13 L_x$.

The above results are based on taking characteristic values. It is possible to extend the arguments to take account of the real non-uniform properties of the jet flow and this will be done in the next section.

The basic directionality patterns predicted by the theory are also of interest. Figures 3 and 4 give directionalities for the self and shear noise, respectively. Only the shear noise pattern of Equation (3) has been plotted, modified by including $\alpha^2 = \epsilon^2 = 0.1$ in the convection term C. The plots have been normalized on the average power emitted at low speeds, so that the plots give the relative contributions of sources of various convection velocities at various angular locations, on the assumption that the Lighthill model for the radiation of convected eddies holds (see Section 6.0).

3.0 NOISE SOURCE LOCATION IN A JET EXHAUST

Equation (1) showed that the sound power per unit volume was given by a proportionality

$$I \sim \frac{u_e^4 M^4 \alpha}{a} \quad (12)$$

where the convection factor and irrelevant constants have been dropped. The parameter α is the ratio of dissipation scale to spatial scale, and is a fundamental property of a turbulent eddy. It is probably a weak function of Reynolds number. The variation of α over the flow is somewhat conjectural. Ribner (References 8-12) has taken α as constant. Lilley (Reference 7) took a variable α and this is supported by the work of Davies, Fisher and Barratt (Reference 10). For the initial studies reported here α was taken as constant. The effect of a variable α assumption is discussed in Section 8.0. This constant α assumption leaves the term $(u_e U)^4$ as the dominant factor in the noise radiation.

New jet turbulence data has recently been taken by Dr. B. J. Tu at Wyle Laboratories, and this data can be used to find the location of the maximum sources. Figure 5 gives, on a reduced scale, the results of some lateral traverses across the jet. Both mean axial velocity, longitudinal turbulence intensity, and their product is shown. The product $(u_0 U)$ is the leading term in the expression for noise generation and can therefore be regarded as a measure of the acoustic effectiveness of the jet.

The purpose of the present report is to discuss the acoustic properties of the jet, so that the aerodynamic data will not be reviewed in detail here. Precautions have been made to ensure that the aerodynamic data is reliable, and the data is generally in reasonable accord with the result of other investigators. The data will be presented in detail in a later report by Dr. Tu.

Figure 6 gives a contour plot of the acoustic effectiveness of a turbulent jet. This is based on the curves of Figure 5, and gives contours of $40 \log_{10} (u_0 U)$. The data is nondimensionalized against the maximum value recorded; in the present case, this occurred at a ridge line spanning from 4 to 6 diameters along the axial direction. Figure 7 gives a contour plot of the mean velocity in the jet. Superimposed on this is the locus of acoustic maxima from Figure 6. It is clear that the data show a dominant source location generally between 0.7 and 0.8 of the exhaust velocity. This is much higher than the $0.5 U_j$ figure often assumed.

It is shown in Section 2.0 that the shear noise has identical functional dependence on the local aerodynamic parameters as the self noise. Hence the source location plots given in Figure 6 applies equally well to the shear noise. It may be noted that the relation between turbulence and mean shear, Equation (9), appears to be unlikely to hold in the transition region. Nevertheless, it is of some practical value to interpreting source location results.

As shown by Figure 5 the location of maximum source strength is somewhat inside the peak turbulence intensity position, simply because of the increased mean velocity at that point.

Two acoustic effects have not been included in the plots of Figures 5 and 6. These are the effects of scale and volume. Because the jet is cylindrically symmetric, outer regions contain more volume and are therefore somewhat more effective than shown in Figure 6. Figure 7 also includes an adjusted line of maximum intensity which incorporates the volume effect. The effect of scale is more difficult to determine and will be discussed further below.

A second feature of importance in Figure 6 is that the flow downstream of the potential core is seen to be a significant generator of noise. The potential core corresponds to the first five diameters of the exhaust flow. Significant noise generation is seen to occur for the first ten diameters of the jet. This finding is of considerable relevance to jet noise prediction.

In order to study the effect further, the integral

$$\int_0^{\infty} (U u_0)^4 \frac{y}{R} d\left(\frac{y}{R}\right) \quad (13)$$

was evaluated graphically from the data shown for each station. This integral gives the overall acoustic effectiveness of the station in question. The results, non-dimensionalized by overall power, are shown in Figure 8.

Figure 8 gives three sets of results. These correspond to three different assumed scaling laws. Equation (6) or (7) has an inverse dependence on scale. The smaller eddies radiate more efficiently. Thus, the overall acoustic effectiveness of each slice of a jet is dependent on the scale assumed. In the initial mixing region, and far downstream in the developed region, scale varies linearly with distance down the axis. The squares on Figure 8 give the acoustic power per diameter based on a uniform linear increase in scale. This assumption is unlikely to be appropriate in the transition region downstream of the potential core. Laurence's results (Reference 16) actually show that scale is decreasing in this area. But as Ribner (Reference 8) remarks, "Even approximate determinations (of scale) are very difficult at these large distances; the instrumental low-frequency cutoff introduces an error that becomes increasingly hard to correct for." Furthermore, Davies, et al. (Reference 15) suggest Laurence's one wire measurement method was invalid in that regime. Nevertheless, it does seem probable that turbulent scales will not vary much through the transition region. The circles on Figure 8 show the sound power per diameter on the assumption of uniform scale throughout the jet.

Perhaps the best physical guess at scale is that it will increase linearly through the initial region, remain constant through the transition region, and then increase linearly again (at a different rate) in the fully developed region. The triangular points in Figure 8 give the source distribution based on this assumption. These points will be taken as the theoretical reference.

Also shown on Figure 8 is experimental evidence on source location due to Eldred (Reference 17). He gives two curves. One is based on the direct measurement of the sound immediately outside the jet stream, and the other represents an attempt to correct these results for refraction which will give an effective source displacement. This refraction corrected curve is probably the best experimental evidence available on source location.

It can be seen that the experimental and theoretical predictions are in close agreement. Sound per unit distance is approximately constant over the initial region. A shallow peak is found near the end of the potential core, and the sound power reduces beyond this point, with acoustic efficiency falling off rapidly beyond about 10 diameters. Theory and experiment are not in agreement about the exact rate of fall off, but this is of minor consequence because acoustic efficiency here is, in any case, low.

Ribner (Reference 19) and Dyer (Reference 20) have previously studied the source location problem, applying simple dimensional arguments based on theory. This gives the well known x^0 and x^{-7} laws for the initial and fully developed region, respectively. It can be seen that the x^0 law is in close agreement with both experiment and the present theoretical calculations. This is not surprising since the simple dimensional dependences assumed for the initial mixing region do agree with experimental evidence. This can be seen in the straight line nature of the velocity and sound contours near the exit in Figures 6 and 7.

The x^{-7} law is more debatable. Undoubtedly the assumed dimensional dependences must occur sufficiently far downstream. The key question is what happens in the transition region. As pointed out by Ribner (Reference 8) and others, although the x^0 and x^{-7} laws do have firm foundation the relative levels of the two cannot be defined simply. The present theoretical approach does overcome this problem, and shows how the one law melds into the other. The initial part of the transition region does not obey an x^{-7} law because it is far from approaching similarity. From an analysis of the acoustic data, Eldred (Reference 18) suggested, "the more intense turbulence generated in the mixing region adjacent to the core does not decay as fast as the mean jet centerline velocity. Therefore, the primary generation of noise in this transition region probably results from turbulence developed upstream and convected downstream, rather than from locally generated turbulence which follows local flow parameters."

The turbulence data and theoretical calculations presented here concur completely with Eldred's conclusions. Figure 9 shows the jet maximum velocity, and maximum intensity as a function of downstream distance.

The maximum velocity occurs along the jet center line while the maximum turbulence intensity occurs in the region of maximum shear in the initial region and on the center line in the developed region. For the present jet it appears that the mean velocity approached similarity (x^{-1} law) at about 8-9 diameters, broadly in line with other investigators. On the other hand, the turbulence intensity had not reached similarity at 12 diameters, the maximum axial distance studied here. Extrapolation suggests that the intensity would reach similarity at 15-16 diameters. That is, the turbulence takes about twice as long to settle down to a similarity law. Other investigators have reported similar trends, although Laurence (Reference 17) finds a quicker approach to similarity.

Beyond 16 diameters, the x^{-7} law for the acoustic source power would apply, but the reasons for the departures from this law in the transition region are now clear, and correspond with the reasoning of Eldred quoted above.

The results above also enable the overall acoustic power radiated to be calculated. If the sound power parameter is integrated along the jet, substitution into Equation (1) gives the result for the noise

$$W = 0.043 \alpha^4 \frac{\rho_0 U^8 D^2}{c^5} \quad (14)$$

where it was assumed that $\alpha = 0.147 x_1$ in the initial region, and a multiple of 1.65 has been used to allow for the shear noise as discussed above. A figure of interest here is that the potential core region (up to 5 diameters from the nozzle) produces about 40 percent of total noise, according to the present calculation.

The constant coefficient $0.043 \alpha^4$ can be identified with the so-called Lighthill's parameter for jet noise radiation (Reference 3). The value of α is a fundamental parameter of the turbulence in a jet, and it has been measured experimentally. Ffowcs-Williams (Reference 5) suggests $\alpha = 0.25$, which gives the constant as 1.9×10^{-4} . This value appears to be based on the uncorrected value of α originally given by Davies, et al. (Reference 15). The correct value is 0.167 for low speed jets, giving the constant coefficient as 3.3×10^{-5} . Lighthill (Reference 3) analyzed acoustic data to give an empirical value of 3×10^{-5} for jets with low initial turbulence level, as have been used to generate the present aerodynamic data. Agreement is extraordinarily good. The result is an asymptotic value for low speeds. The effect of the C^5 term will be to increase the efficiency substantially at supersonic speeds, following the curves of Figures 1 and 2. It is not possible to account for this in the present integrated approach in any simple way, but the effects will be discussed in Section 5.0.

4.0 CALCULATION OF THE FREQUENCY SPECTRUM

The spectral theory by Pao and Lawson (Reference 6) gives also the power spectral density for the noise generated by a unit volume of turbulence. The frequency dependence is

$$I(x_0, \omega) \sim \omega^4 e^{-\mu \beta^2 \omega^2} \quad (15)$$

where β is the turbulence time scale and μ equals 1.0 for shear noise and 0.5 for self noise. The respective locations of peak noise frequency are $\sqrt{2}/\beta$ for shear noise and $2/\beta$ for self noise at low convective speed. For sources moving at higher convective speeds, the Doppler shift factor C^{-1} should be included. The time scale β relates to the spatial scale through

$$\beta = \alpha / \alpha M_c c \quad (16)$$

The turbulence scale α varies along the axis of the jet linearly, with a possible exception in the transition zone, as discussed in the previous section. Hence, each section of the jet, at different axial locations, will produce sound with a different peak noise frequency. Furthermore, the spectral distribution of the noise from each segment will follow Equation (15) if a Gaussian isotropic turbulence model were chosen.

Using Equations (15) and (16), together with the source distribution results obtained in the previous section, the spectrum of the self noise and the shear noise can be computed. The shear noise has exactly the same spectrum as the self noise, except for a half octave shift of the peak frequency location. Furthermore, its power is known to be approximately half of that of the self noise. Hence, it is necessary to compute only the self noise starting from the basic data obtained so far in this study.

The peak frequency of self noise, $1/\beta$, for a small turbulence volume, can be non-dimensionalized as a Strouhal number, fD/U . Using Equation (16) for β and taking $\alpha = 0.147 x_1$, the Strouhal number for the peak frequency is found to be

$$S = \frac{2\alpha}{0.147 x/D} \left(\frac{M_c}{M} \right) \quad (17)$$

where M_c/M can be taken as 0.8 which corresponds to the convective speed in the maximum noise source zone. The peak noise frequency at the five diameter station is chosen as a reference. The jet is subdivided into segments having peak frequencies at $1/3$ octave intervals from the reference frequency. The source segments can be subdivided in different ways depending on the variation of the turbulence scale. In Figure 10, the solid line subdivision follows from assuming that the turbulence scale varies linearly from 0 to 5.5 diameters, remains constant from 5.5 to 8 diameters, and

increases linearly again from 8 diameters onward. A second subdivision, denoted by the dotted lines, is obtained by assuring that the turbulence scale increase linearly throughout the length of the jet.

The noise produced by each segment of the jet is calculated in one-third octave band levels according to Equation (15). The normalized one-third octave band level distribution of Equation (15) is shown in Figure 11. The overall one-third octave band levels of the self noise, shear noise, and their sum are given in Figure 12.

In both methods of noise source subdivision, the peak of the overall noise is close to a Strouhal number of 0.30, which is a good agreement with jet noise measurements. However, the overall spectrum predicted by the second method of subdivision (i.e., the turbulence scale varies linearly throughout the jet) indicates a broad peak, a 8.0 dB/octave rise on the low frequency side, and a 5.0 dB/octave decline on the high frequency side. This spectrum agrees almost exactly with those of the SAE standard and the Potter and Jones measurement (Reference 26).

The agreement of the prediction with acoustic data does not necessarily imply that the second method of subdivision is better than the first. The reasons for which the first method failed to produce a smooth shaped spectrum are the compound of the following items:

- The turbulence scale in the transition zone is assumed to be constant. This zone occupies a width of 2.50 diameters in the region of maximum noise production and is responsible for nearly 30 percent of the overall sound power from the jet. Furthermore, the entire segment produces noise with the same peak frequency which corresponds to a Strouhal number of approximately 0.30.
- The "weighted Gaussian" spectrum, Equation (15), has a relatively narrow spectrum. The deficiency in high frequency content is particularly prominent.

The combination of these two factors causes the predicted spectrum to take a higher peak and drop off faster at both ends.

However, according to some preliminary data obtained by Dr. B. J. Tu at Wyle Laboratories, the frequency spectrum in the transition region has a profile very much similar to the overall jet noise spectrum which has a wide peak region and declines slowly at the high frequency end. In such a case, the "linear-constant-linear" turbulence scale rule will indeed predict an overall noise spectrum in close agreement with the acoustic measurements. Clearly, further experimental data on various spectral and integral parameters of the jet turbulence structure in the transition region are necessary for more detailed predictions of jet noise spectrum.

5.0 EXTENSIONS TO THE SUPERSONIC CASE

Direct use of the Lighthill-Ffowcs Williams results to extend the present calculations to supersonic speeds leads to two important difficulties. Firstly, although the U^8 and U^3 asymptotic laws are correctly predicted by the theory it also predicts a major increase in acoustic output at around $M=1$ (see Figures 1-4). No such increase has yet been observed in practice. Secondly, the theory basically predicts a frequency spectrum whose peak increases with velocity because of the Doppler shift, while experiment finds a lowering of peak frequency. The so-called "reverse Doppler shift" is well known.

It appears that these divergences can be accounted for by the effects of refraction and mitigation of convection. These are discussed in the next section. Before developing these ideas it is worthwhile to study the supersonic case in a little more detail. Consider again the basic parameter dependence of Equation 1.

$$I \sim \frac{U^4 u_0^4 \alpha^4}{a C^5}$$

The effect of the convection factor C^{-5} has already been discussed (see Figures 1-4), but the other parameters in the equation also have an important effect on the noise generation.

To understand the possible effects at supersonic speeds it is helpful to return to the basic derivation of the results. The sound is governed by the $\partial^2 T_{ij} / \partial t^2$ term.

T_{ij} is proportional to u_0^2 so that the intensity is proportional to u_0^4 . The U^4 term arises from the $\partial^2 / \partial t^2$ differentiation, but the reason why it arises is of interest.

A jet retains approximately the same geometric structure as velocity is increased, at least at subsonic speeds. Thus, the spatial scales of the turbulence remain roughly constant, but the fact that the geometric shape is the same means that the time scale must reduce in direct proportion to the velocity. Thus, the basic rates of change of stress increase as velocity increases. The eddies therefore become more acoustically efficient by a factor of U^4 as speed increases. Note that this is not a function of convection or of any basic acoustic phenomenon; it is a consequence of the experimental fact that jet geometry remains constant.

The most significant effect of supersonic speeds on jet geometry is that the core length increases. In other words, the basic time scales increase at supersonic speed, so that, by the above arguments, efficiency reduces. This appears to be a basic physical effect not included in simple dimensional analysis of supersonic flow which could explain why experimentally measured efficiencies at sonic speeds are lower than predicted by theory.

Unfortunately, detailed application of this concept to a practical case leads to problems. Equation (1) has an α^4 term in the numerator which does reduce at supersonic speeds. But the C^{-5} term behaves almost identically as α^{-4} at supersonic speeds so that the direct effect of time scale cancels. Figure 13 shows the integral of $\alpha^4 C^{-5}$ as a function of Mach number. It can be seen that α has no direct effect at supersonic speeds, while at subsonic speeds, the α^4 variation dominates. Thus, it is necessary to look for further explanations. The basic physical reasoning described in the last paragraph seems correct and in accord with the theory. One possibility results from the observation that the supersonic radiation is essentially in the form of highly directional Mach waves. Thus, substantial nonlinear attenuation might be expected, and indeed shadowgraph pictures of supersonic flows appear to show very rapid attenuation of radiated shocklet patterns (Reference 21). This would lead to a more important contribution of the time-variant components which should follow the reduction noted above.

Lighthill (Reference 2) originally suggested that the reduced acoustic efficiency at supersonic speeds occurred because of reduced turbulence intensity. Indeed an acoustic radiation damping was postulated. More recent work has tended to de-emphasize this effect, principally because the observed acoustic power levels (1/2 percent of available mechanical power) seem to be too low to have any substantial effect on the turbulence. If nonlinear acoustic attenuation is included then possibly radiation damping could be effective because very large near field acoustic energy could be dissipated during propagation to the point of observation.

No definitive measurements of turbulence intensity at supersonic speeds appear to be available, so that we must rely on theoretical considerations. Modern thought on supersonic turbulence appears to be inclining towards the hypothesis originally advanced by Morkovin (Reference 22) that turbulent structure is unaffected at supersonic convection. Only turbulent velocities approaching sonic speed might be expected to show any substantial effects of compressibility. Maise and MacDonald (Reference 23) showed Morkovin's hypothesis to be acceptable for a supersonic boundary layer. Donaldson and Gray (Reference 24) applied a form of Morkovin's hypothesis to a wide range of the exhaust flows, and did find a small change of the mixing parameter with Mach number. Their mixing parameter was determined empirically, but with considerable consistency, from a wide range of jet flows. It seems that their results should be applicable to supersonic jet noise prediction via the use of a simple model for turbulent scales.

6.0 LIMITATIONS

Several authors have pointed out that the basic Lighthill model for the jet noise must break down at sufficiently high frequencies. The model calculates the acoustic output of quadrupole sources in a uniform acoustic medium at rest. The sources are allowed to move, but the medium into which they radiate does not. This model is acceptable for either low convection Mach numbers, or low frequencies with wavelengths much larger than the jet dimension. It is clear that sound of sufficiently high frequency will radiate into the local convected medium of the jet stream, and the effect of convection will then be to refract the sound already formed rather than to augment the sound power in any direct way. Thus, the convection factor will not apply at high frequencies, and the loss of its effect is intimately connected with the appearance of directionality effects due to refraction.

It is difficult to specify the frequency at which these effects occur. Fridred (Reference 18) showed, from an extensive data analysis, that the directivity patterns for a jet were governed by refraction even down to the frequencies of peak acoustic output, and this would argue the absence of convection effects there. Support for this viewpoint comes from a consideration of the near field effects of a quadrupole. Simple dimensional analysis suggests that the near field (r^{-6}) terms of a quadrupole are equal to the far field terms (r^{-2}) in intensity after as little as $1/36$ of a wavelength from the source, while the mid field (r^{-4}) terms are equal to the far field after $1/2$ of a wavelength. It can be argued that convection effects change near field non-radiative terms into far field radiative terms. Thus, wavelengths smaller than six times a characteristic dimension in the jet should show a lessened effect of convection. This gives a limiting Strouhal number $f D/U \sim 1/2 M$. Typical peak acoustic frequencies correspond to $f D/U \approx 0.2$ for low speed jets ($M < 1$). The arguments thus again suggest that convection effects could be absent even quite close to the peak frequencies in the jet.

Increase of jet speed will have two effects. From the formula above convective effects will be less significant. But the basic strength of the convective effects increases rapidly with speed (see Figures 1 and 2). Following the arguments above, this will only affect the low frequencies. Thus, one could expect the lowest frequencies in the jet to increase rapidly with speed. Since the lowest frequencies are predominantly radiated by the large scale downstream region where velocities are lower, the effect would depend on some fraction of the exhaust Mach number. The strong increase in efficiency of the lower frequencies due to this effect affords a partial explanation of the lowering of the characteristic acoustic frequency (from $f D/U \sim 0.2$ to $f D/U \sim 0.02$) with increase in exhaust speed. Of course, the slower rates of mixing at supersonic speeds must also contribute to this result.

It may be noted that the removal of the convective effects at high frequencies does not affect the basic U^8 law. As discussed in the last section, this results from the experimentally observed reduction in turbulence time scale with increase in velocity. This does raise the problem of supersonic convection. The low frequency sound,

which dominates the supersonic flow, will follow the U^3 law in this region since its source mechanism closely resembles the Lighthill-Ffowcs Williams model. But according to the present arguments the U^8 law should still apply to the high frequencies apart from the reduction due to the slower mixing rate at supersonic speeds. The authors consider that nonlinear acoustic attenuation effects provide the answer to this problem, and it is hoped a later study will provide quantitative estimates of the effect.

7.0 EXPERIMENTAL RECOMMENDATIONS

Analysis of the theory suggests several relevant experiments both aerodynamic and acoustic. The study of the inhomogeneous jet suggests that the dominating effect in jet acoustics is jet nonuniformity. Each part of the jet radiates with a different efficiency and a different frequency. It appears to be more important to include this effect in a prediction technique than to consider fine details of the individual local radiation patterns. Thus, knowledge of the mean velocity, turbulent intensity, and scales throughout the jet should enable good predictions of noise to be made. Mean velocity and turbulent intensities are reasonably well established, but the variation of scale in the jet is not. The only comprehensive data is that of Lawrence, but it is difficult to accept this data for a major portion of the jet. Thus, a thorough study of local scales could be of extreme value (see Section 8.0).

The same arguments can be reapplied to more complex exhaust configurations often used to reduce noise at source. Multiple nozzles, coaxial flows, and various vented arrangements are included in this category. Little knowledge of the turbulent intensities and scales exists for these configurations. Such measurements could provide considerable insight into the causes of observed reductions in jet noise, and should lead to improved designs for silencing devices. Study of the parameters of deflected exhaust flows should also be of value.

A turbulence effect of both acoustic and more general interest, which has not been widely reported, is that intensities in a direction of about 45 degrees outward from the jet axis are almost a factor of two greater than intensities for components directed at 45 degrees inward. When it is recalled that sound is proportional to T_{ij} , the component of the stress tensor in the direction of the observer, it is clear that this effect could lead to directional noise peaks of the order of 10 db. This provides an alternative explanation of the lobed sound patterns observed in a jet. A survey of the jet to demonstrate the orientation of the components of maximum intensity would be of great interest since information on this effect does not exist. It should be reasonably straightforward to extend the acoustic theory to incorporate this feature.

Several acoustic experiments are also suggested by the theory. It is clear that no complete evaluation of existing data utilizing theoretical knowledge has been carried out. An interesting attempt in this direction was performed by Lush (Reference 14). The referenced paper reports several data correlations of comparatively minor value but Figure 6 of that reference is of extreme interest and is reproduced here as Figure 14. Lush attempted to separate out the shear and self noise contributions, took the Jones form of Lighthill's shear directivity (Equation 4), and examined many acoustical spectra at both the angle of maximum intensity and at this angle plus 52.5 degrees. Spectra were normalized on the usual Strouhal number basis, but including the Doppler frequency shift factor C . Thus, frequency spectra were referred back to the basic turbulence mechanisms.

The collapse of spectra, shown in Figure 14, is astonishingly good by jet noise standards. A surprising feature is that the two spectra differ by about 3 octaves in peak frequency. The shear noise and self noise spectra would be expected to peak at different frequencies. The self noise must peak higher because it is basically due to the square of the turbulence while the shear noise is directly proportional. Ribner (Reference 8) predicted an octave difference, and Pao and Lawson (Reference 6) a half octave difference. Chu (Reference 25) showed the difference to be slightly over an octave via experimental measurements of turbulence, but no mechanism to suggest a separation anywhere near three octaves has been suggested.

The effect appears to be due to the lack of accounting for refraction. Ribner and MacGregor (Reference 12) show the results via a diagram reproduced here as Figure 15. The shear noise has a strong peak along the axis due to its basic directionality and the convection factor, and the self noise, a small peak due to convection. The spectra of both have a higher basic frequency content along the axis due to the Doppler shift. However, in addition the shear noise contribution dominates near the axis while the self noise dominates near 90 degrees. This leads to a slightly lower peak frequency along the axis than at 90 degrees for the joint spectrum. Refraction preferentially redirects the high frequencies away from the axis, resulting in a strong "reverse" Doppler shift with the highest frequencies observed at 90 degrees. Now Lush's data has been "Doppler corrected". Thus, an observed plot of Figure 15 would be "corrected" to give a result with very substantial frequency separation between the noise near the axis and at 90 degrees, as shown in the last plot of Figure 15. The effect would be still further accentuated in Lush's plot, Figure 14, by the use of one third octave plots. The spectrum is sharper near the axis than at 90 degrees, so that peak percentage bandwidth levels would be more separated than the peak levels per cycle. The effects noted above would not be as pronounced at the maximum power location chosen by Lush, but do appear to provide an explanation for his data.

Extensive acoustic data evaluation following the methods of Voce and Lush, or Ribner and MacGregor seems to be long overdue. The Ribner-Pao-Lawson directivity patterns suggest that the best way to separate the shear and self noise contributions is to compare spectra near the axis and at 90 degrees. At 90 degrees the shear noise is predicted to be zero, while it should dominate near the axis. The arguments above suggest strongly that refraction must be accounted for in the analysis if meaningful results are to be found. Fortunately, Ribner's group has now developed substantial theoretical and experimental data which allow refraction effects to be evaluated. Refraction corrections near the axis are large so that it may be desirable to choose a location nearer 45 degrees as suggested by Ribner and MacGregor for the collapse.

Several further effects should be determinable from proper data analysis. The theoretical peak efficiency near sonic speeds is a major stumbling block in application. Gross experimental data on sound power has never revealed a peak, but equivalent effects may be observable in a more detailed study. Analysis of sound

power in narrow bands as a function of Mach number should be most helpful. Low frequency noise is unaffected by refraction or nonlinear effects and should obey the theoretical predictions accurately. Thus, a peak in the low frequency power curve should be anticipated. The occurrence of such a peak in the analysis is a crucial test of the basic theory, and its nonoccurrence would force re-examination of fundamentals.

Lighthill (Reference 2) claimed that a peak could be observed at small angles to the axis where the Doppler correction is at its strongest. But no detailed verification of this statement has been published. Several published curves of velocity exponent as a function of field position do not provide an adequate test because the variation of power is not given over a wide range of convection Mach numbers. Curves of sound pressure level at various angles as a function of exit velocity would be of great value in determining basic mechanisms.

Proper analysis of the acoustic data can also give basic information about the aerodynamic parameters governing the acoustic radiation. Voce and Lush (Reference 14) give a curve of α against Mach number that is in fair agreement with trends that can be inferred from Donaldson and Gray's aerodynamic data (Reference 24). Once the source input terms are properly established, the definition of a prediction technique of wide range and good accuracy should be straightforward. Furthermore, the same forms of analysis can be used to show the predominant mechanisms of noise generation and suppression in more complex flows, and thus aid the design of effective silencing devices.

8.0 EFFECT OF THE SCALE RATIO

The space-time scale ratio α appears in the basic equation (1) raised to the fourth power, and thus plays a vital role in determining the magnitude of the noise radiated. In this report α has been taken as a constant over the jet. This appeared to be a simple initial assumption and agreed with the assumption of Ribner. However other assumptions could be more realistic and are discussed in this section.

The basic definition of α is

$$\alpha = \frac{L_x}{U L_t} \quad (18)$$

where

L_x is the spatial scale

and L_t is the dissipation time scale.

The assumption $\alpha = \text{constant}$ corresponds to assuming that the local ratio of space to time scales is dependent on local mean velocity. This is difficult to see physically as the turbulent eddies have no means of knowing what their local velocity is, relative to the undisturbed air. The eddies should be aware of the local mean shear or the local turbulent velocity, so that it should be more acceptable to use these as the non-dimensional parameters.

Davies, Fisher, and Barratt (Reference 16) found experimentally,

$$L_t = 3.8 \left(\frac{\partial U}{\partial x} \right)^{-1} \quad (19)$$

$$L_x = 0.13 x_1 \quad (20)$$

which gives

$$\alpha \sim \frac{x}{U} \frac{\partial U}{\partial x_2} \quad (21)$$

showing a dependence of α on mean shear.

Lilly (Reference 7) used an expression of this type to give a formula for the shear noise radiation of the jet

$$I \sim c^{-5} \left(\frac{\partial U}{\partial x_2} \right)^6 u_0^2 \quad (22)$$

and this was used by Davies, Fisher, and Barratt to define source locations in a jet. A basic objection to equations of this form of (21) and (22) is that they must be

misleading beyond the end of the potential core where turbulence intensity is a maximum on the axis at the point of zero shear. Davies, Fisher, and Barratt also found a relation between turbulence intensity and mean shear

$$u_0 = 0.2 L_x \frac{\partial U}{\partial x_2} \quad (23)$$

and using this gives

$$\alpha = 0.13 \frac{u_0}{l} \quad (24)$$

This result, that the scale ratio is proportional to the non-dimensional turbulence intensity, has an attractive feel about it, and should be valid all over the jet. Substitution in the basic equation for jet noise leads to the result

$$I \sim \frac{u_0^8}{a} \quad (25)$$

that is; the noise output is proportional to the turbulence intensity to the eighth power. This appears to be an important result since it is independent of the local scale α , and has obvious implications for noise suppression. Any given device can be evaluated via a local measurement of turbulence intensity, with no requirement for time consuming measurements of space and time scales.

The basic result (25) will also change some of the details of source location given earlier in the report. The most notable effects will be that the lines of maximum noise intensity of Figures 6 and 7 will lie along the line of maximum turbulent intensity at around $U = 0.5 U_0$. The axial source location of Figure 8 will show a stronger weighting of the downstream portions since the turbulence intensity approaches similarity more slowly than the mean velocity (see Figure 9). This will result in a closer agreement between prediction and Eldred's experimental results of Figure 8, and will produce somewhat more emphasis on the lower frequency end of the frequency spectrum.

The integral result of close agreement between the theoretical and experimental values of the Lighthill parameter should not be substantially changed by the change in assumption. Derivation of the actual values will be left to a later report. Similarly the other general discussion should be unchanged.

At supersonic speeds the direct effect of α disappears as shown in Figure 13. The basic noise dependence is then

$$I \sim \frac{u_0^4}{U}$$

where the U in the denominator arises from the asymptotic M^{-5} law of the C^{-5} term. Thus according to the present model the scale ratio α has little effect either at subsonic or supersonic speeds.

9.0 CONCLUSIONS

The principal conclusions of this study are:

1. The characteristics of noise radiation from an exhaust flow are governed by the local variation of gross parameters such as turbulence intensity and scale. Details of wave number frequency spectra are of secondary importance.
2. Shear noise produces approximately half the sound power but double the peak sound pressure of self noise.
3. The initial mixing region roughly follows the x^0 law for intensity.
4. The transition region produces 60 percent of the sound power, and a shallow peak in sound production occurs near the end of the potential core (5 diameters).
5. Final similarity and the x^{-7} law only occurs beyond about 15 diameters.
6. Axial source location results are in good agreement with experimental data.
7. The empirical relation of Davies, et al., between mean shear and turbulence intensity suggests that shear noise has the same local dependence as self noise.
8. Integration gives the theoretical value of the Lighthill parameter K in the equation $W = K c^{-5} \rho_0 U^8 D^2$ as 3.3×10^{-5} compared with the empirical value of 3×10^{-5} for low speed jets.
9. Predicted one third octave band noise spectra show good agreement with the SAE standard spectrum.
10. The calculations of the spectrum indicate that more precise information on turbulence scales in the transition region are necessary for accurate jet noise spectrum predictions.
11. Theory predicts a major increase in sound power as speed increases into the transonic and supersonic speed ranges. This is not observed experimentally.
12. Aerodynamic effects, notably the lengthening of the core will reduce source strength at supersonic speeds, but the most important reason for the discrepancy appears to lie in the neglect of refractive and nonlinear effects in the theory.
13. It appears possible to analyze acoustic data in a more systematic fashion. Analyses versus Mach numbers as a function of frequency and angular location will provide crucial tests of theoretical predictions.

14. Self and shear noise can be separated following the concepts of MacGregor and Lush. This may be particularly valuable for the analysis of suppressor configurations, and also offers the promise in inferring aerodynamic parameters, such as scale, from acoustic data.
15. A physically reasonable model for the ratio of space to time scales suggests that local noise intensity is directly proportional to turbulence intensity to the eighth power.
16. Detailed experimental information on turbulence parameters is required. The local scale parameters represent the most significant unknown feature. Variations induced by complex flows, for instance suppressor nozzles, are also essentially unknown.
17. Theory does provide the basis for a comprehensive prediction technique for jet noise, particularly as the acoustic and aerodynamic information suggested in items 14-16 becomes available.

REFERENCES

1. Lighthill, M. J., "On Sound Generated Aerodynamically I., General Theory," Proc. Roy. Soc. Vol. A211, 564-578 (1952).
2. Lighthill, M. J., "On Sound Generated Aerodynamically II, Turbulence as a Source of Sound," Proc. Roy. Soc., Vol. A222, 1-21 (1954).
3. Lighthill, M. J., "The Bakerian Lecture, 1961. Sound Generated Aerodynamically," Proc. Roy. Soc., Vol. A267, 147-182 (1962).
4. Lighthill, M. J., "Jet Noise," Wright Brothers Lecture, AIAA J., Vol. 1, 1507-1517, (1963).
5. Ffowcs-Williams, J. E., "The Noise from Turbulence Convected at High Speed," Phil. Trans. Roy. Soc., London, Vol. A255, 469-503 (1963).
6. Pao, S. P. and Lawson, M. V., "Spectral Techniques in Jet Noise Theory," Wyle Laboratories Research Report, WR 68-21 (1969).
7. Lilley, G. M., "On the Noise from Air Jets," Aeronautical Research Council Report, ARC 20, 376, N.40, F.M. 2724 (1958).
8. Ribner, H. S., "The Generation of Sound by Turbulent Jets," Advanced in Applied Mechanics, Vol. 8, 103-182, Academic Press (1964).
9. Ribner, H. S., "Quadrupole Correlations Governing the Pattern of Jet Noise," Univ. of Toronto, Inst. for Aerospace Studies, UTIAS Report No. 128 (1967).
10. Atvars, J., et al., "Refraction of Sound by Jet Flow on Jet Temperature," University of Toronto, Inst. for Aerospace Studies, UTIAS Report No. 109 (1965).
11. Grande, E., "Refraction of Sound by Jet Flow and Jet Temperature, II," University of Toronto, Inst. for Aerospace Studies, UTIAS Report No. 110 (1966).
12. Ribner, H. S. and MacGregor, "The Elusive Doppler Shift in Jet Noise," The Sixth International Congress on Acoustics, Paper No. F-3-8, Tokyo, Japan (1968).
13. Lee, R., et al., "Research Investigation of the Generation and Suppression of Jet Noise," General Electric Co., Flight Propulsion Lab. Report, prepared under Navy Bureau of Weapons Contract No. AS 59-6160-C (1961).
14. Voce, J. D. and Lush, P. A., "An Application of Quadrupole Theory to Correlate the Directivity and Spectra of High Speed Jet Noise," AGARD Conference Proceedings, No. 42, (1969).

15. Jones, I. S. F., "Aerodynamic Noise Dependent on Mean Shear," *J. Fluid Mech.*, Vol. 33, 65-73 (1968).
16. Davies, P.O.A.L., Fisher, M.J., and Barratt, M.J., "The Characteristics of the Turbulence in the Mixing Region of a Round Jet," *J. Fluid Mech.*, Vol. 15, 337-367, Corrigendum, p.559, (1963).
17. Laurence, J. C., "Intensity, Scale, and Spectra of Turbulence in Mixing Region of Free Subsonic Jet," NACA Report 1292, Lewis Center Flight Propulsion Laboratory (1956).
18. Eldred, K. M., et al., "Suppression of Jet Noise with Emphasis on the Near Field," Technical Report ASD-TDR-62-578, Flight Dynamics Laboratory, Wright-Patterson AFB (1963).
19. Ribner, H. S., "On the Strength Distribution of Noise Sources Along a Jet," University of Toronto, Inst. of Aerophysics, UTIA Report No. 51 (1958).
20. Dyer, I., "Distribution of Sound Sources in a Jet Stream," *J. Acoust. Soc. Am.*, Vol. 31, 1016-1021 (1959).
21. Lawson, M. V. and Ollerhead, J. B., "Visualization of Noise from Cold Supersonic Jets," *J. Acoust. Soc. Am.*, Vol. 44, 624-630 (1968).
22. Morkovin, M. V., "Effects of Compressibility on Turbulent Flows," Proceedings of the Marseille Conference on Turbulence CNRS Report No. 108, Paris, 367-380 (1962).
23. Maise, G. and McDonald, H., "Mixing Length and Kinematic Eddy Viscosity in a Compressible Boundary Layer," *AIAA J.*, Vol. 6, 73-80 (1968).
24. Donaldson, C. duP. and Gray, K. E., "Theoretical and Experimental Investigation of the Compressible Free Mixing of Two Dissimilar Gases," *AIAA J.*, Vol. 4, 2017-2025 (1966).
25. Chu, W. T., "Turbulence Measurements Relevant to Jet Noise," University of Toronto, Inst. for Aerospace Studies, UTIAS Report No. 119 (1966).
26. Potter, R. C. and Jones, J. H., "An Experiment to Locate the Acoustic Sources in a High Speed Jet Exhaust Stream," Paper presented at the 74th Meeting of the Acoustic Society of America, November 1967.

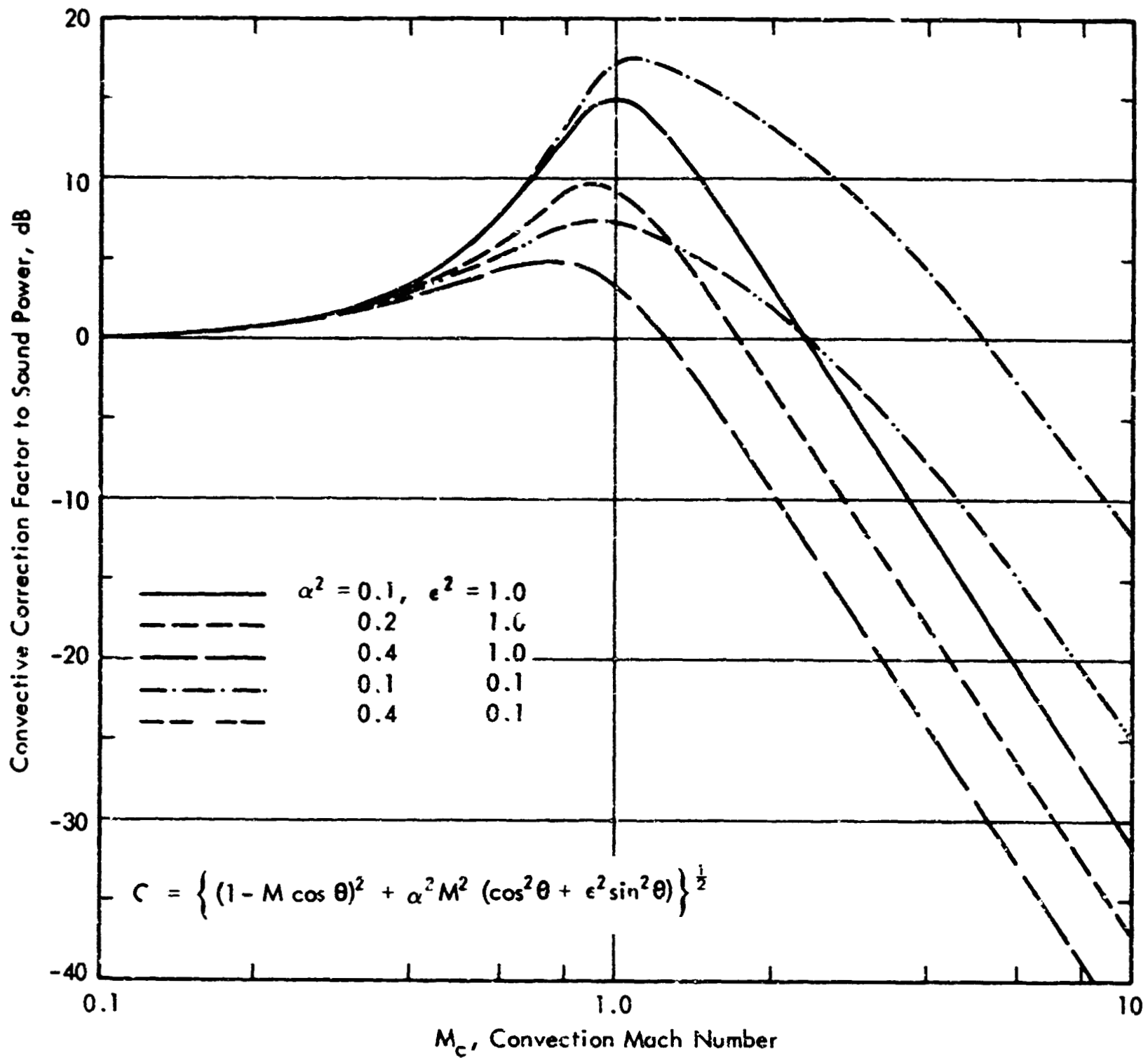


Figure 1. Spherical Average of the Self Noise Convection Factor,

$$\frac{1}{4\pi} \int_0^{2\pi} C^{-5} \sin \theta \, d\theta, \text{ in dB Relative to its Value at Zero}$$

Mach Number for each Given Set of Parameters α^2 and ϵ^2 .

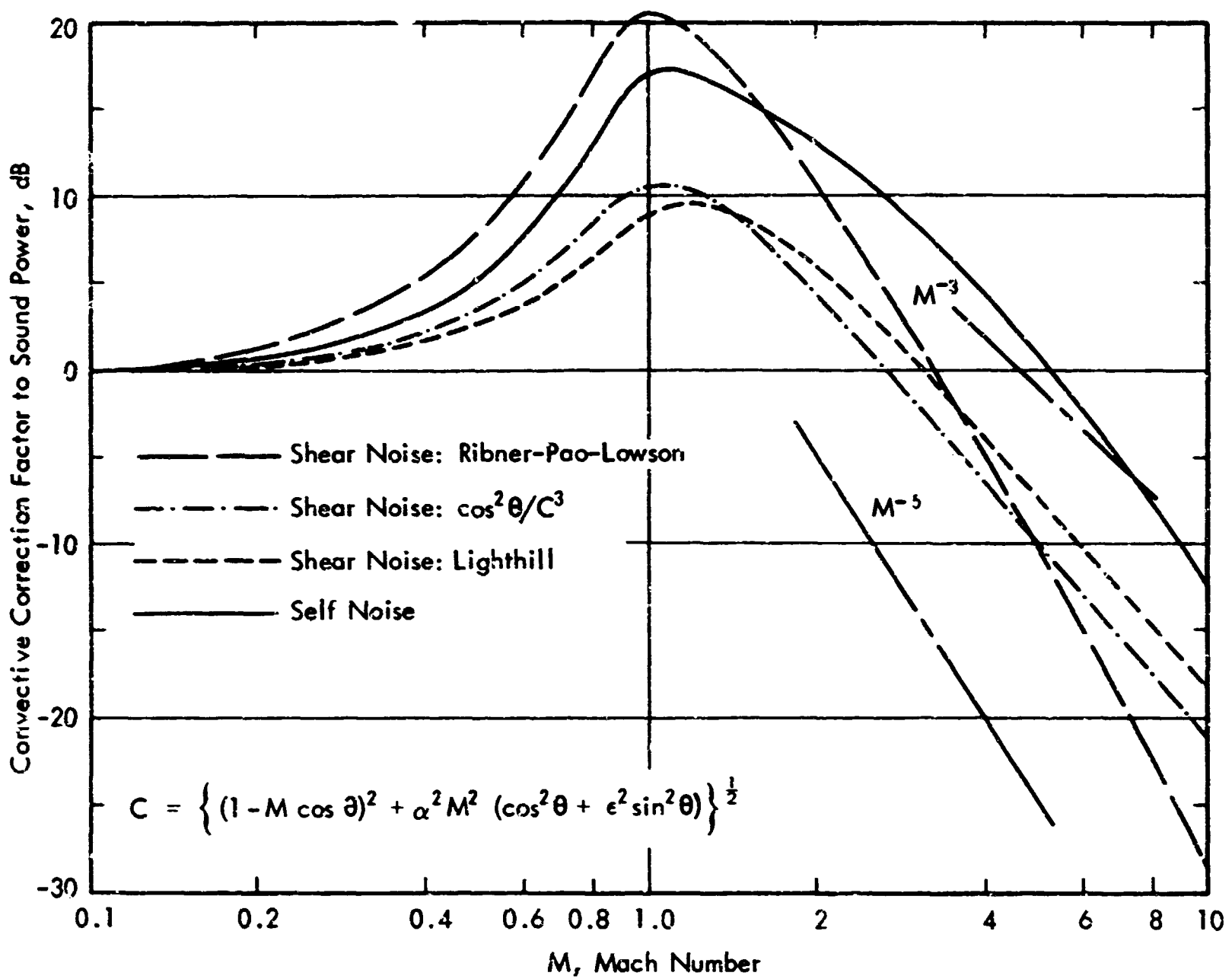


Figure 2. Spherical Average of the Shear Noise Convection and Directivity

Factor, $\frac{1}{4\pi} \int_0^{2\pi} C^{-n} \Phi(\theta) \sin \theta d\theta$, in dB Relative to its Value at Zero Mach Number for Each Case of Given n and $\Phi(\theta)$. The α^2 and ϵ^2 have a Fixed Value of 0.1.

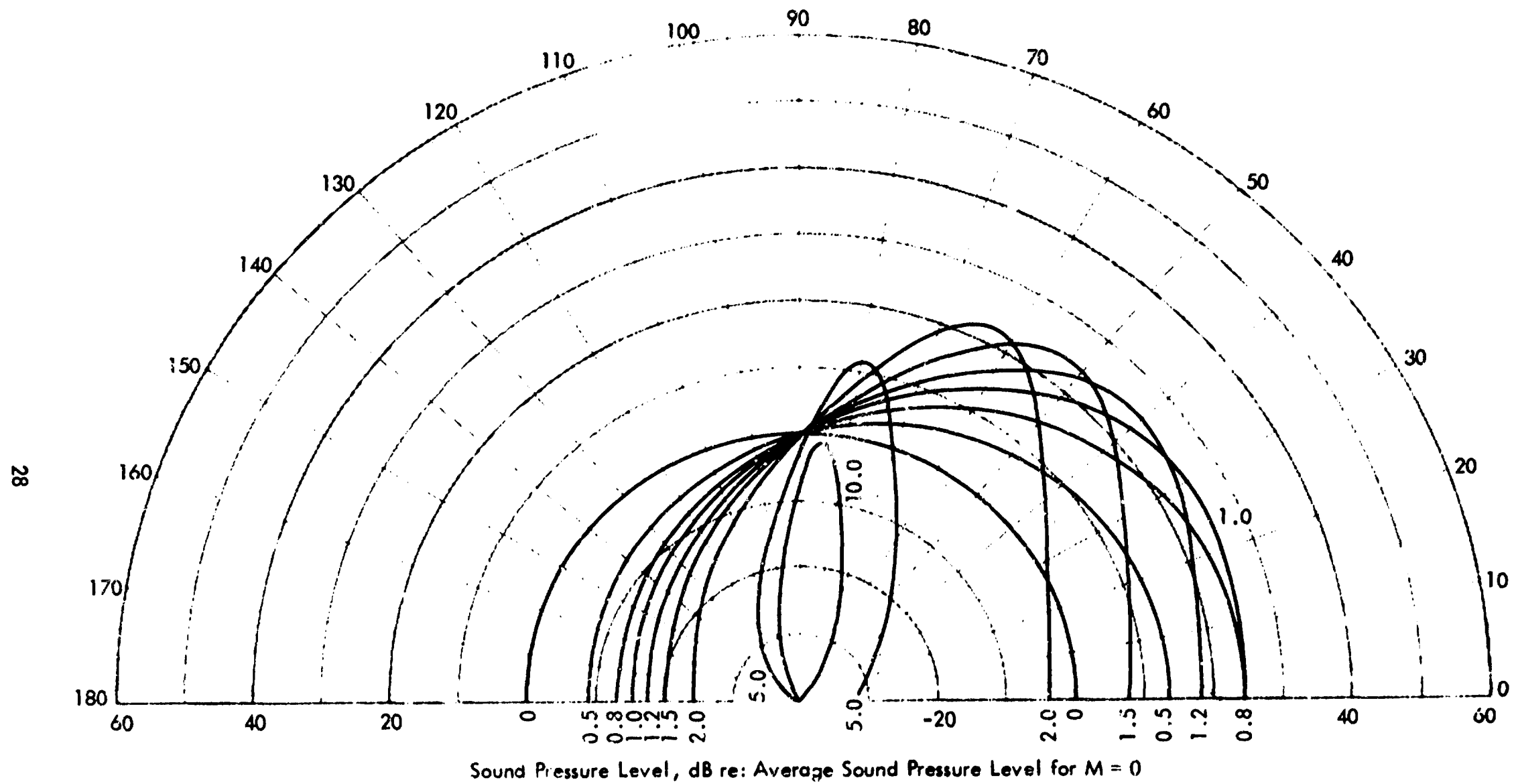


Figure 3. The Self Noise Convection Directivity Factor at Various Mach Numbers. Sound Pressure Levels are Shown in dB Relative to the Average Sound Pressure Level at Zero Mach Number

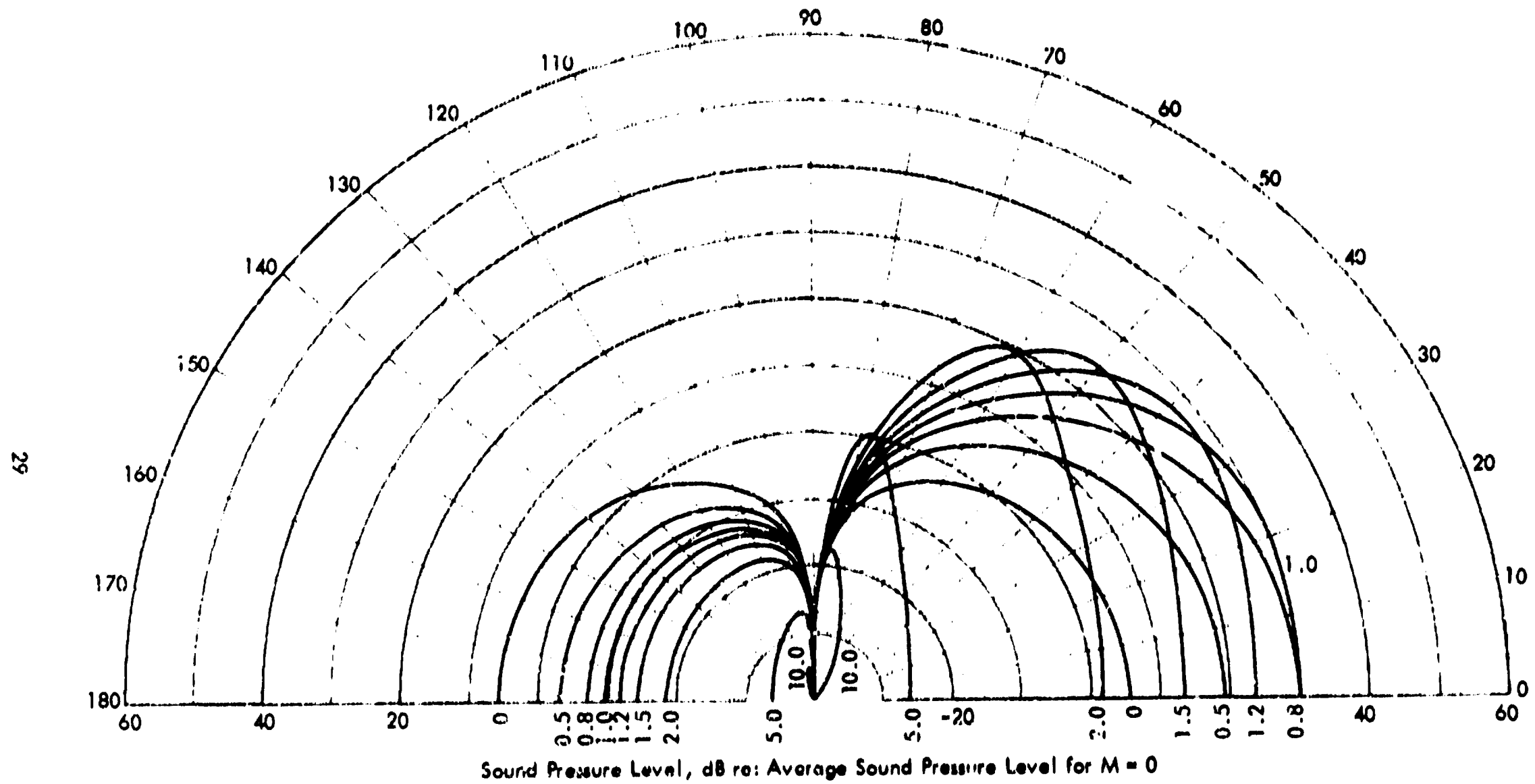


Figure 4. The Ribner-Pao-Lowson Shear Noise Convection Directivity Factor at Various Mach Numbers. Sound Pressure Levels are Shown in dB Relative to the Average Sound Pressure Level at Zero Mach Number

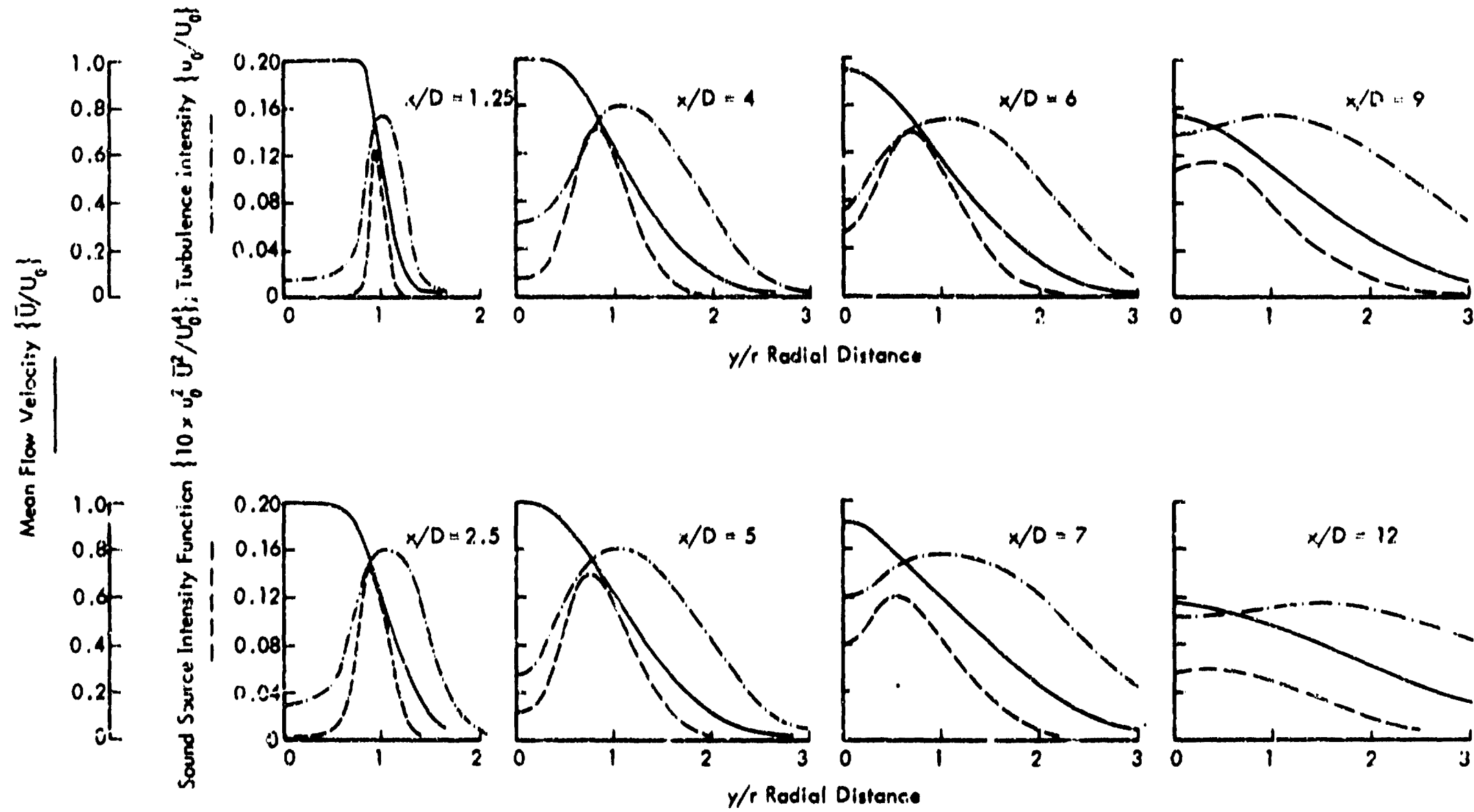


Figure 5. Mean Flow Velocity Profile, Turbulence Intensity Profile, and the Square of their Product at Various Stations along the Axis of a Low Speed Jet Exhaust Flow.

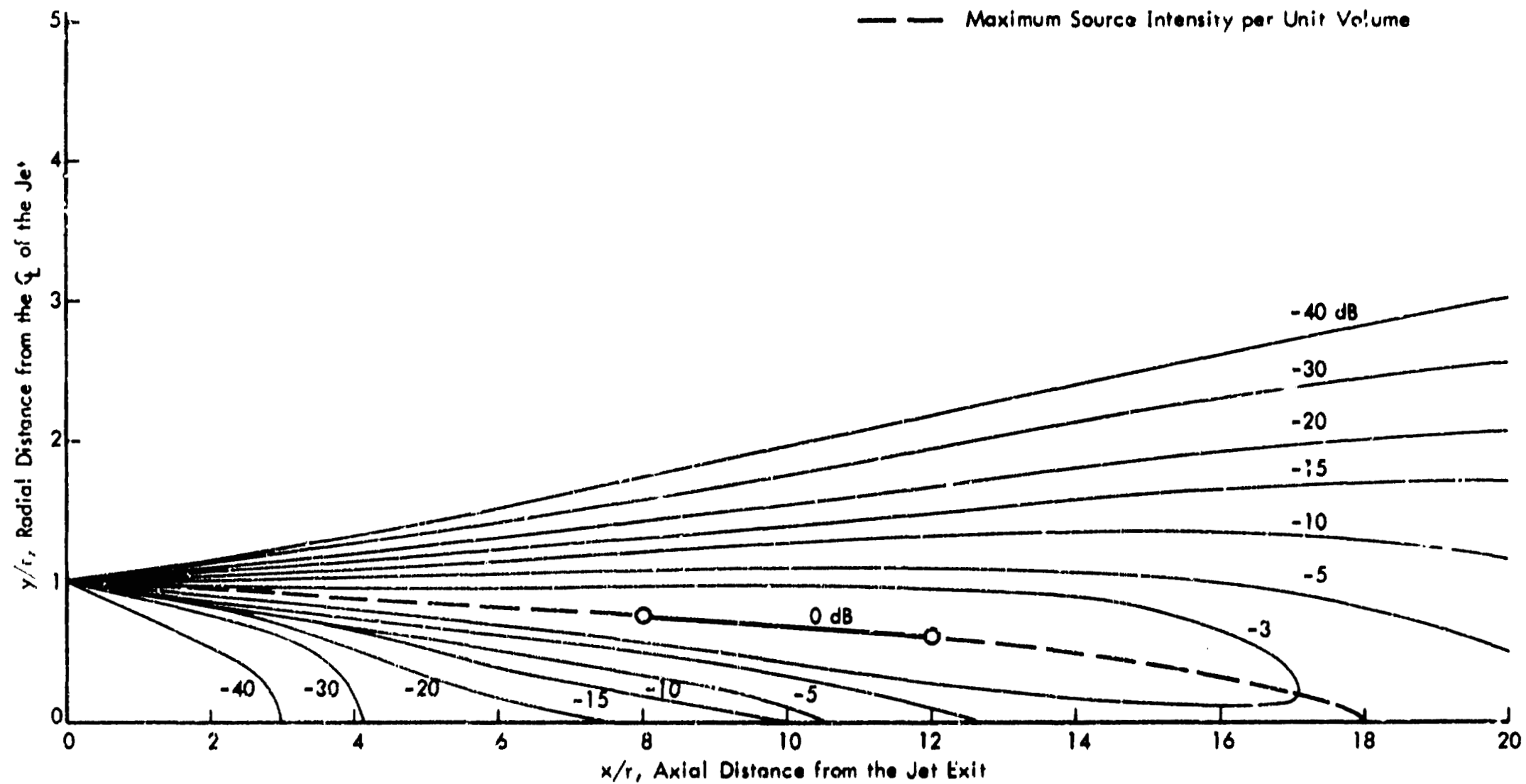


Figure 6. Contours of Noise Source Intensity in a Low Speed Jet Exhaust Stream. The Intensity Levels are shown in dB Relative to the Maximum Noise Intensity

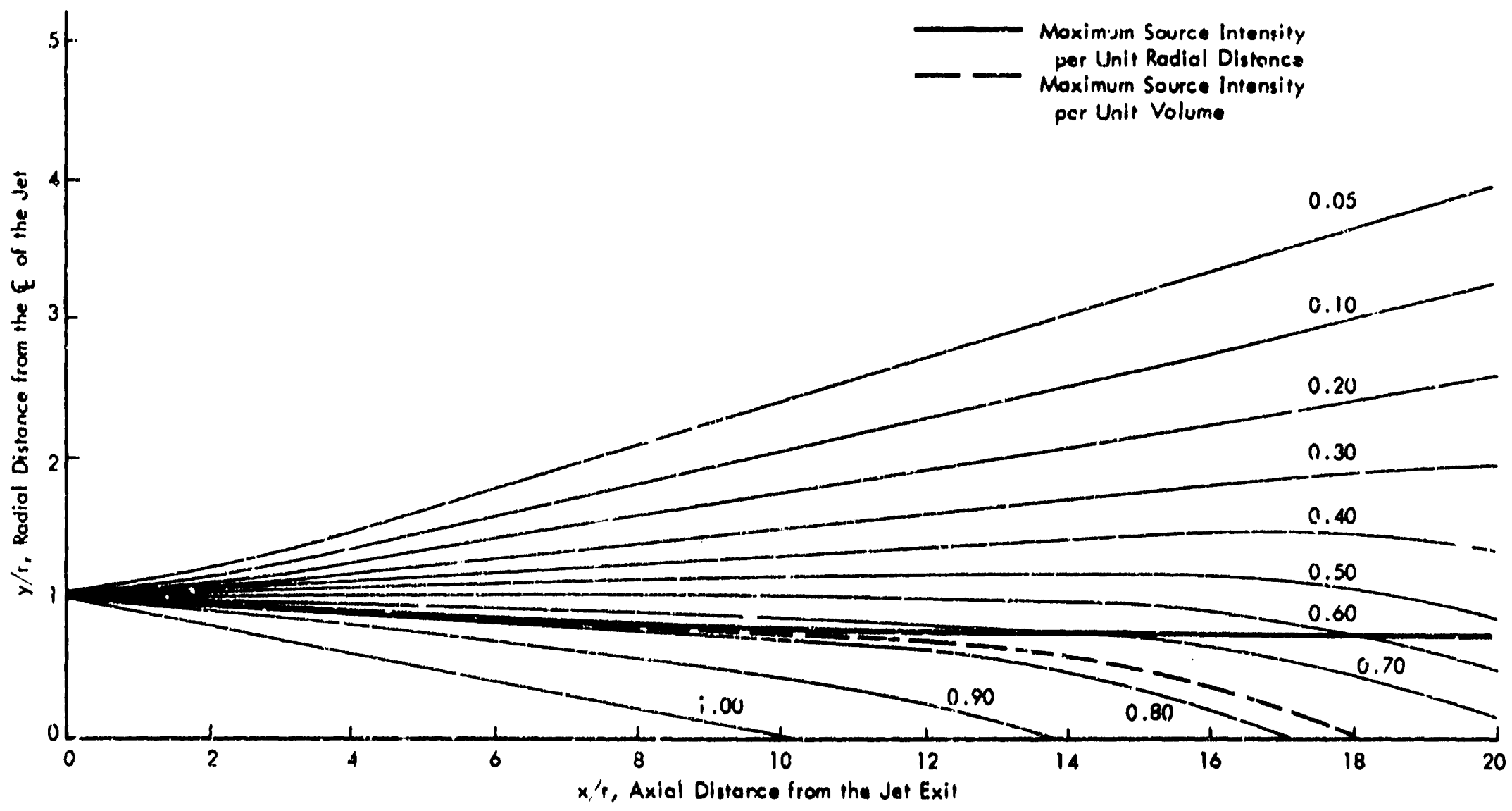


Figure 7. Contours of Local Mean Velocities in a Low Speed Jet Exhaust Stream. The Mean Velocity is Normalized Against the Jet Exhaust Velocity

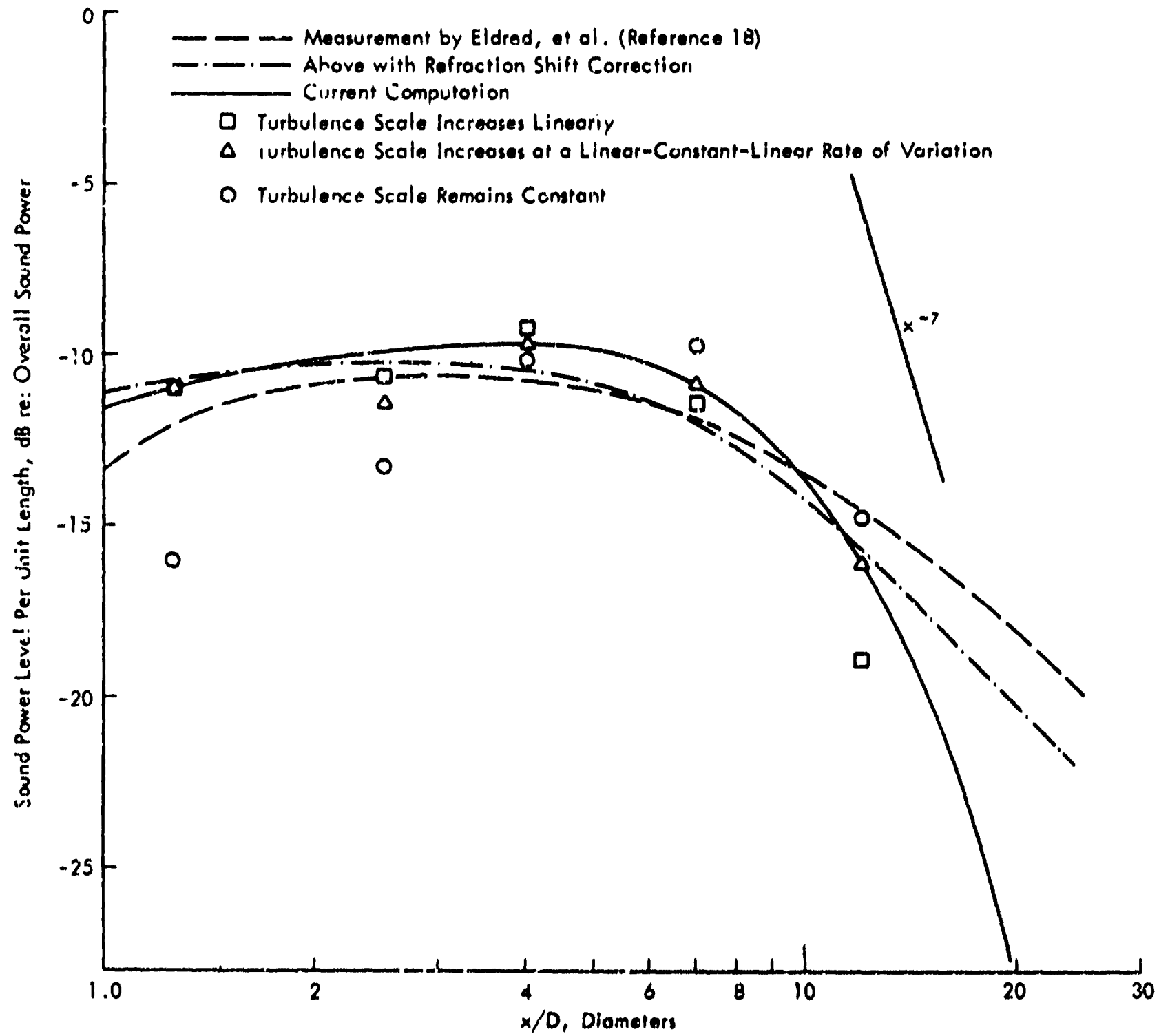


Figure 8. The Integrated Noise Source Strength Per Unit Length Along the Axis of a Low Speed Jet Exhaust Stream

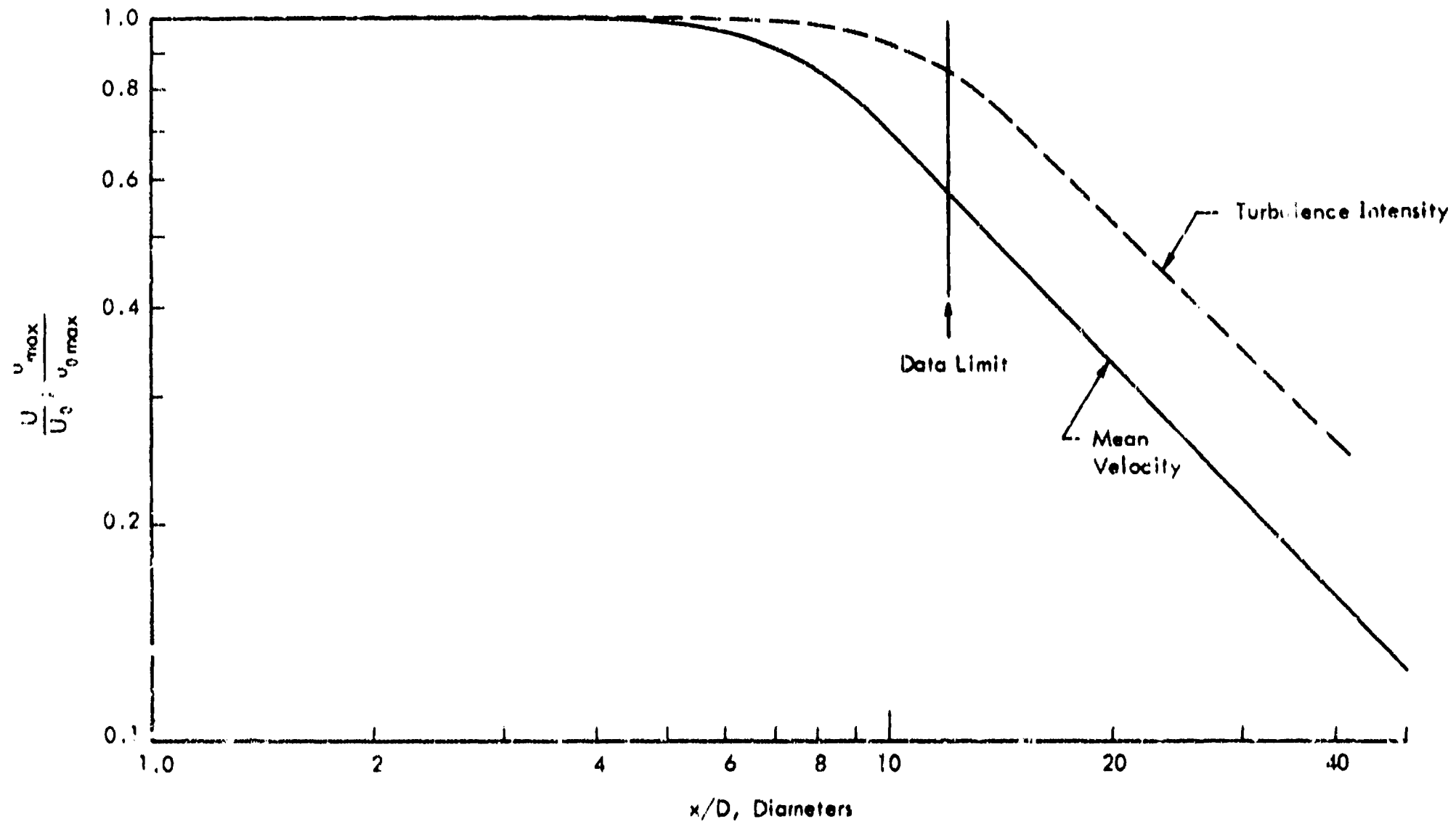


Figure 9. Profiles of Maximum Mean Flow Velocity and Maximum Turbulence Intensity in the Axial Direction of the Jet. The Approach to Similarity Assumes Different Patterns for These Profiles

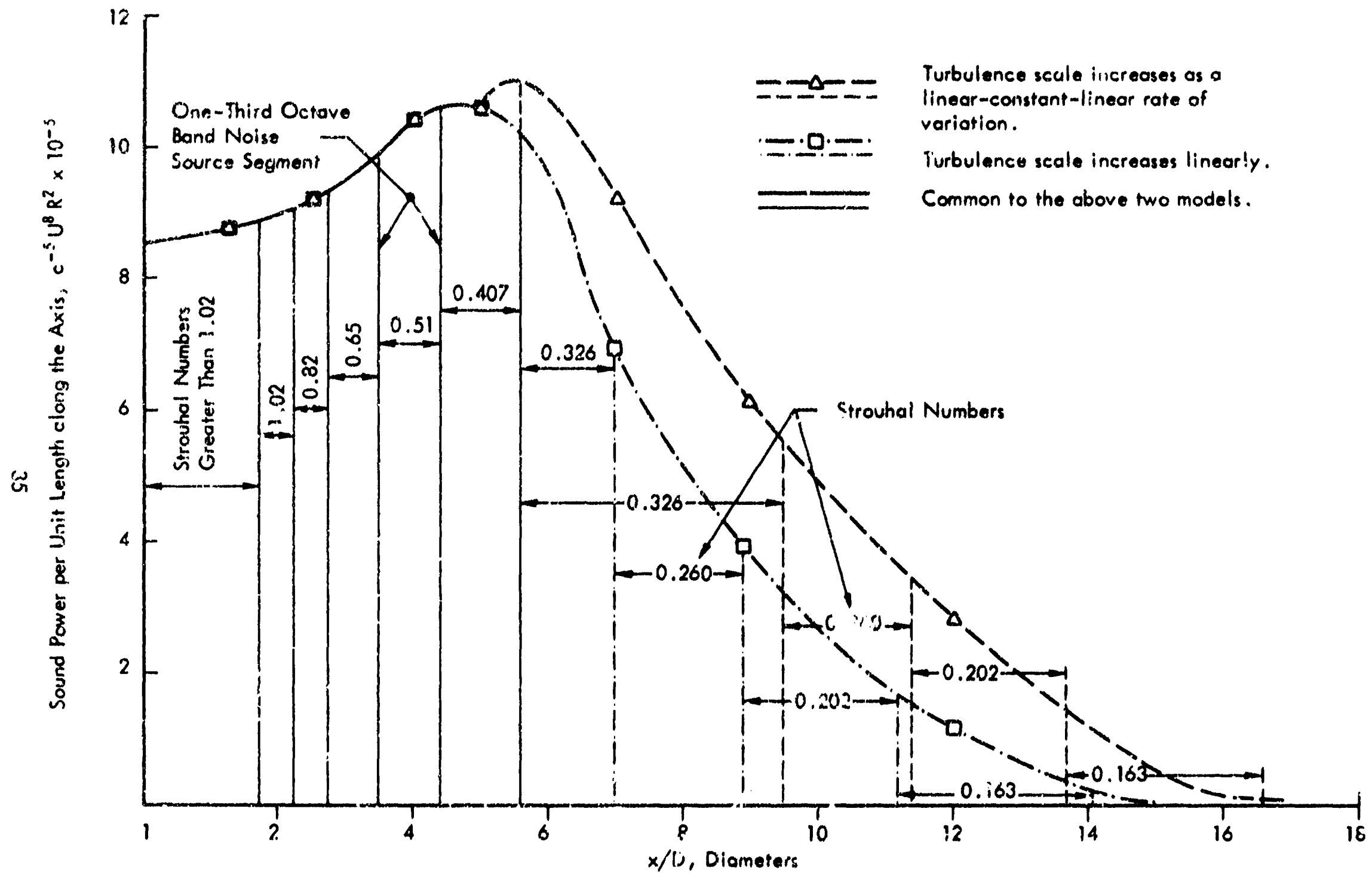


Figure 10. Subdivision of a Low Speed Jet Exhaust Stream According to the Local Peak Noise Frequency. The Difference Between Peak Frequencies in Consecutive Segments is One-Third Octave

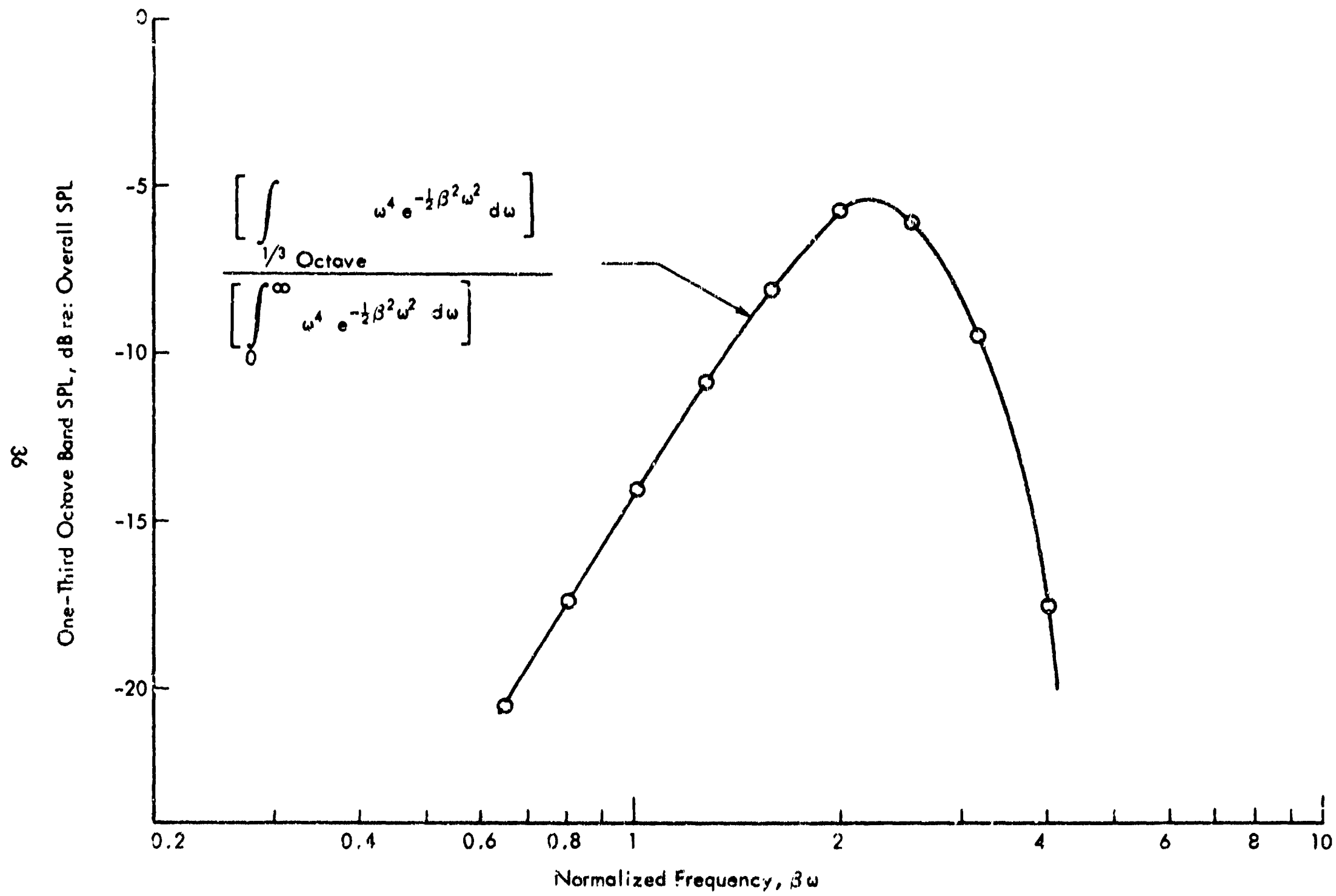


Figure 11. The Normalized One-Third Octave Band Spectral Level of the Model "Weighted Gaussian" Frequency Function

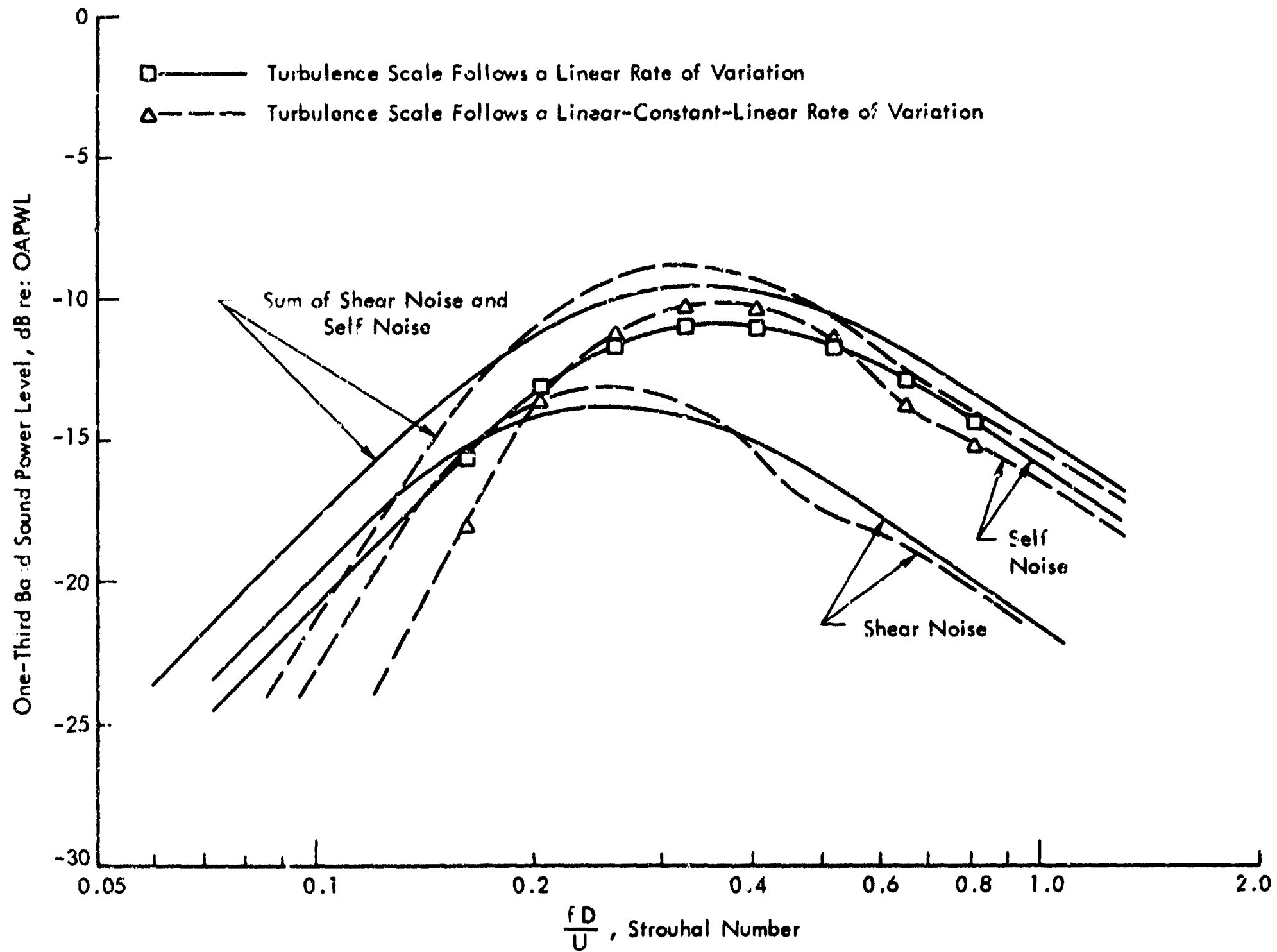


Figure 12. The Predicted Self Noise, Shear Noise, and Overall Noise Spectra for a Low Speed Jet Based on the Pao-Lowson Theory

$$\alpha^4 \int \frac{\sin \theta}{C^5} d\theta$$

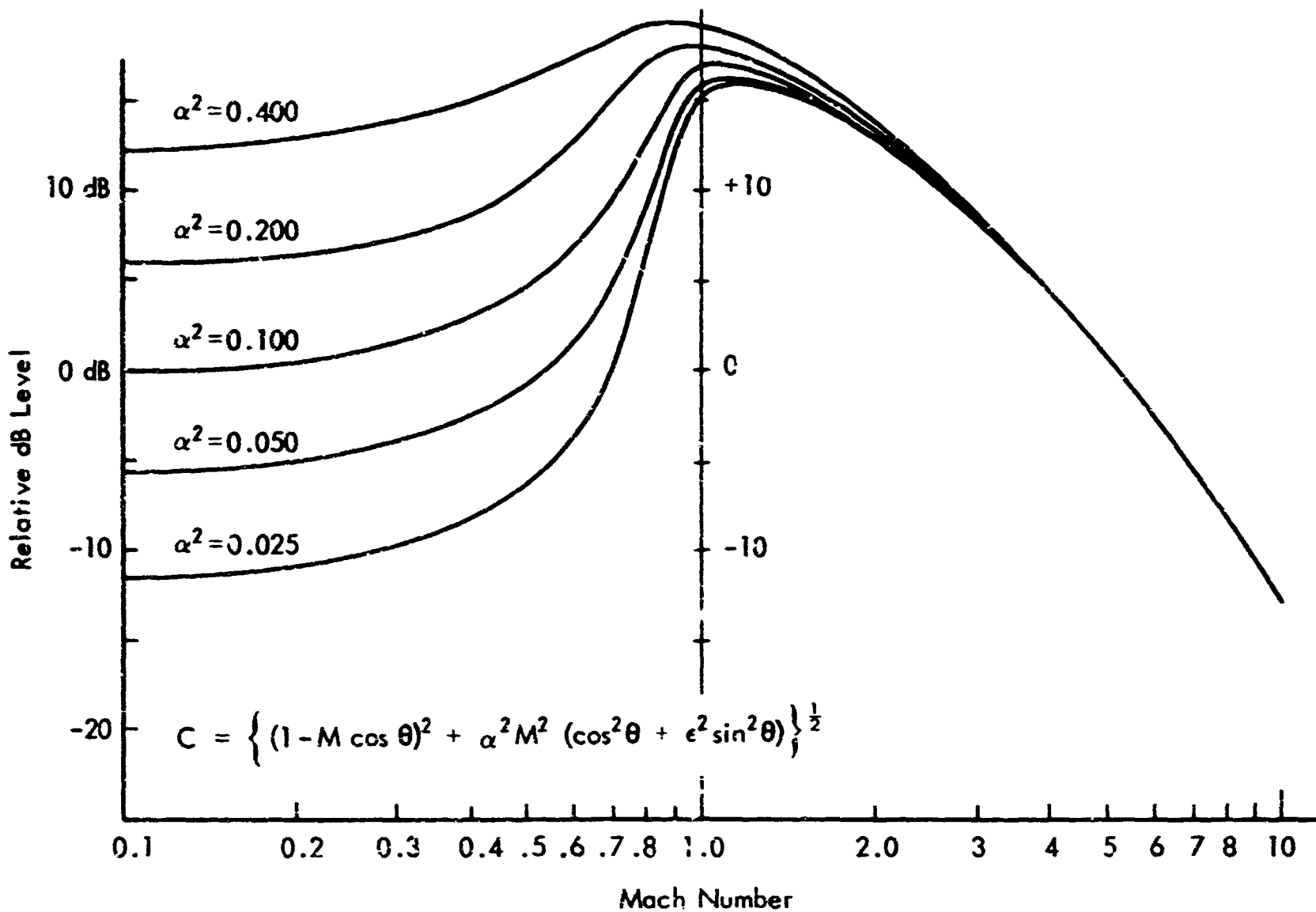
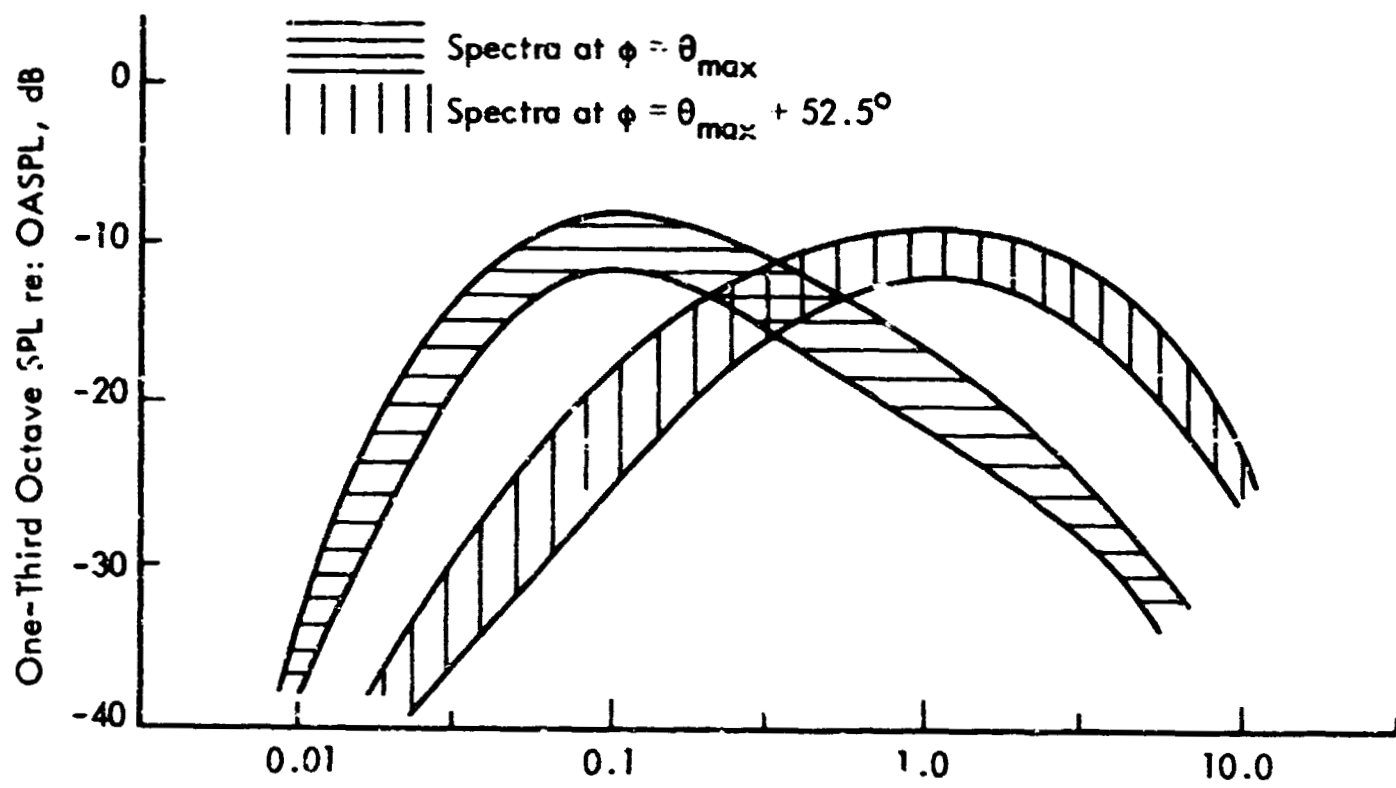


Figure 13. The Value of $\frac{1}{4\pi} \int_0^{2\pi} \alpha^4 C^{-5} \sin \theta d\theta$, in dB Relative to its Value at Zero Mach Number for Each Given Value of α^2 . The Parameter ϵ^2 has a Fixed Value of 0.1



$$\frac{f_{DN}}{V_J} \left[\{1 - M_C \cos \phi\}^2 + \alpha^2 M_C^2 \right]^{\frac{1}{2}}$$

Figure 14. The Two Types of Frequency Spectrum Shown on Normalized Plot (after Voce and Lush, Reference 14)

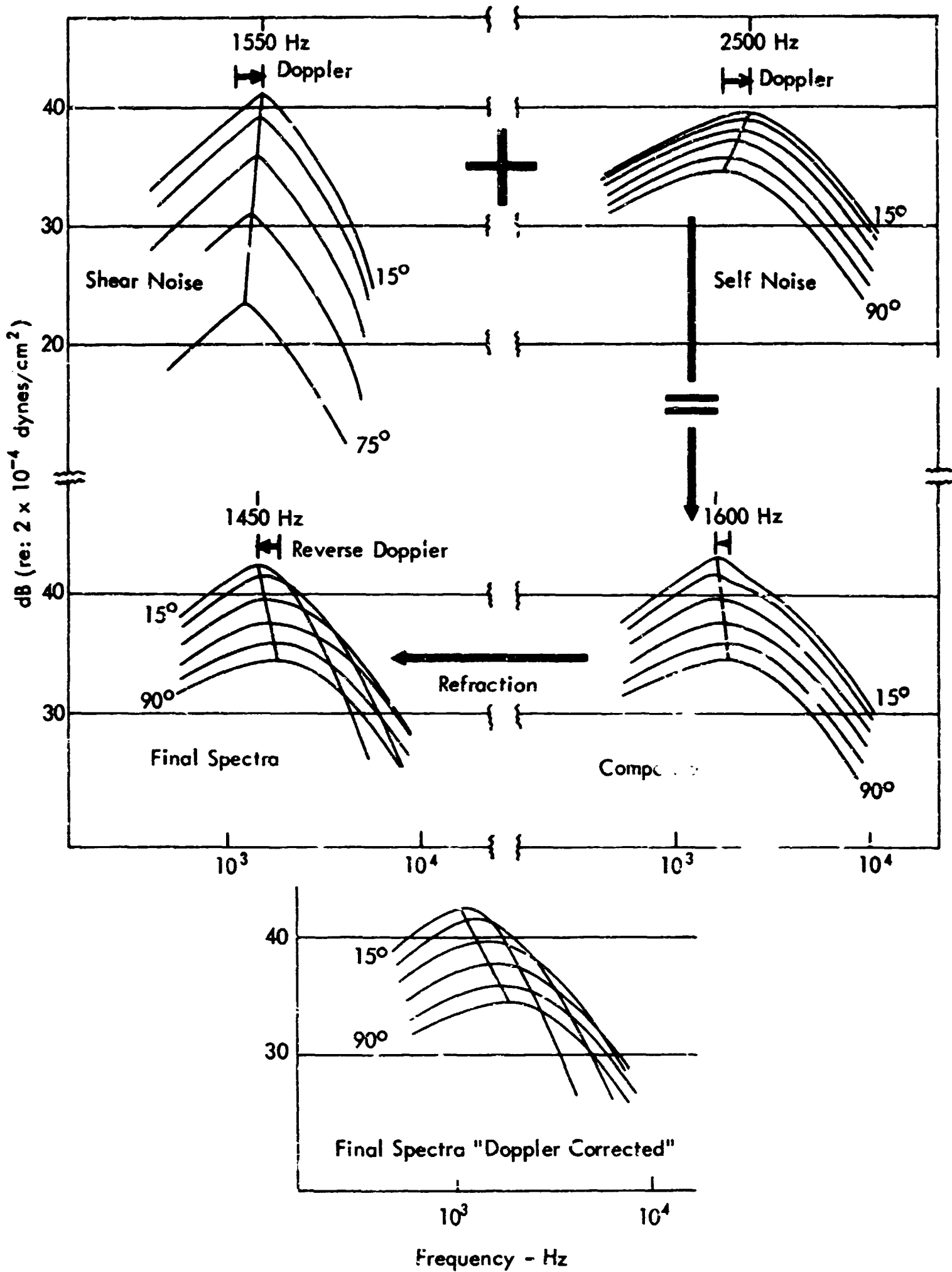


Figure 15. Masking and Apparent Reversal of the Convection-Associated Doppler Shift Illustrated with Experimentally Derived Data (Ribner and McGregor, Reference 12)